

Event-Driven Receding Horizon Control For On-line Distributed Persistent Monitoring on Graphs

Shirantha Welikala and Christos G. Cassandras

Abstract—This paper considers the optimal multi-agent *persistent monitoring* problem defined on a set of nodes (targets) interconnected according to a fixed *graph* topology (PMG). The objective is to minimize a measure of mean overall node state uncertainty evaluated over a finite time interval via controlling the motion of the team of agents. A class of threshold-based parametric controllers has been proposed in a prior work as a *distributed on-line* solution to this PMG problem. However, this approach involves a lengthy and computationally intensive parameter tuning process, which can still result in low performing solutions. Recent works have focused on appending a centralized off-line stage to the aforementioned parameter tuning process so as to improve its performance. However, this comes at the cost of sacrificing the on-line distributed nature of the original solution while also increasing the associated computational cost. Moreover, such parametric control approaches are slow to react to compensate for possible state perturbations. Motivated by these challenges, this paper proposes a computationally cheap novel event-driven receding horizon control (ED-RHC) approach as a *distributed on-line* solution to the PMG problem. In particular, the discrete-event nature of the PMG systems is exploited in this work to determine locally (i.e., both temporally and spatially) optimum trajectory decisions for each agent to make at different discrete event times on its trajectory. Numerical results obtained from this ED-RHC method show significant improvements compared to state of the art distributed on-line parametric control solutions.

I. INTRODUCTION

Continuously monitoring a dynamically changing environment by deploying a team of agents is a scenario that arises in many applications such as environmental sensing [1], surveillance systems [2], energy management [3] and also in data collecting [4]. Such situations are widely studied under the name of *persistent monitoring* problems - aiming to determine the optimum agent behaviors for a desired monitoring task.

While the monitoring tasks in some applications equally value (prioritize) every point in the environment [5], [6], in many others, only a finite set of “points of interest” (henceforth called “targets”) holds a value [7], [8]. The persistent monitoring problem considered in this paper also belongs to the latter class, where the goal of the agent team is to monitor (sense or collect information from) each target to reduce an “uncertainty metric” associated with the target state. Typically this target uncertainty metric increases when no agent is monitoring (or sensing) the target and decreases

when one or more agents are monitoring the target. Also, the effectiveness of such a target monitoring task may depend on the relative locations of the agents and the target. Hence the global objective is to control the agents so as to minimize an overall measure of target uncertainties.

Persistent monitoring problems in 1D environments have been solved using classical optimal control techniques. For such problems, the optimal solutions have revealed that it is sufficient to use a class of threshold-based parametric controllers to control the agents optimally [9]. However, this synergy between optimal control and parametric controllers does not hold for 2D environments [6]. Nevertheless, works in [6], [10] have successfully investigated different shapes of agent trajectories (e.g., elliptical) that can be optimized by manipulating associated shape parameters. Apart from the apparent sub-optimality, failing to react for dynamic changes in target uncertainties and high dependence on the initial target/agent conditions are some drawbacks of such adherence to standard agent trajectory shapes. As a solution to these drawbacks, the recent work [7] has proposed a graph abstraction (where targets are modeled as nodes and inter-target agent trajectory segments are modeled as edges) to formulate the *persistent monitoring on graphs* (PMG) problems.

In PMG problems, an agent trajectory is defined by the sequence of *nodes to be visited* and the *dwell time* to be spent at each visited node. Due to the complexity of this problem, [7] have proposed (yet another) class of threshold-based parametric controllers (TCP), where each agent would enforce a set of thresholds on its neighboring target uncertainty values to make its immediate trajectory decisions: the next target to visit and the dwell time to be spent. Hence this TCP method is *distributed*. The work in [7] has further proposed an *on-line* gradient-based technique to determine the optimum set of thresholds for each agent to use - based on infinitesimal perturbation analysis (IPA). However, as pointed out in [8], this IPA-TCP approach often converges to poor local optimum solutions. The work in [8] has proposed to address this issue by appending an *off-line* and *centralized* threshold initialization scheme to the IPA-TCP method. Even though this modification increases the performance considerably, it now requires a centralized controller and a high computational power (at-least in the off-line phase). Moreover, since its on-line phase is still governed by the IPA-TCP method [7], if some state perturbation occurred, the involved on-line threshold parameter tuning process will take a considerable amount of time to react, and also the subsequent solution obtained can still be a poor local optimum.

*Supported in part by NSF under grants ECCS-1509084, DMS-1664644, CNS-1645681, by AFOSR under grant FA9550-19-1-0158, by ARPA-E's NEXTCAR program under grant DE-AR0000796 and by the MathWorks.

The authors are with the Division of Systems Engineering and Center for Information and Systems Engineering, Boston University, Brookline, MA 02446, {shiran27, cgc}@bu.edu.

Motivated by these challenges, this paper presents an entirely different approach that can be used to solve the same PMG problem. Specifically, the discrete event nature of the PMG systems is exploited here to derive an event-driven receding horizon controller (ED-RHC) to optimally govern each of the agents in an on-line distributed manner using only a minimal amount of computational power.

First, it is shown that each agent's trajectory can be fully characterized by the sequence of decisions it has to make at different (local) discrete-event times. Each such decision defines a subsequent discrete event time where another decision has to be made. Second, considering a generic agent, a generic optimization problem is formulated to determine few subsequent locally optimum decisions to follow. Generally, this optimization problem is non-convex and constrained. As the next step, structural properties of this optimization problem are exploited to derive its solutions in closed form. These closed form optimal decisions fully define the ED-RHC approach. Finally, the proposed ED-RHC method is implemented to solve generic PMG problems and its performance is compared with the IPA-TCP solution.

This paper is organized as follows. Section II presents the problem formulation, some preliminary results and the overview of the ED-RHC solution. Sections III, IV and V respectively presents the formulations and solutions to the three main classes of optimization problems associated with the ED-RHC solution. Finally, simulation results are discussed in Section VI and Section VII concludes the paper.

II. PROBLEM FORMULATION

A. Persistent Monitoring On Graphs (PMG) Problem

Consider an n -dimensional mission space containing M targets (nodes) in the set $\mathcal{T} = \{1, 2, \dots, M\}$ where each target $i \in \mathcal{T}$ is located at a fixed location $Y_i \in \mathbb{R}^n$. A team of N agents in the set $\mathcal{A} = \{1, 2, \dots, N\}$ is deployed to monitor the targets. Each agent $a \in \mathcal{A}$ is allowed to move independently in the mission space and its location at time t is denoted by $s_a(t) \in \mathbb{R}^n$.

a) Target Model: Each target $i \in \mathcal{T}$ has an associated uncertainty state $R_i(t) \in \mathbb{R}$ which follows the dynamics given by

$$\dot{R}_i(t) = \begin{cases} A_i - B_i N_i(t) & \text{if } R_i(t) > 0 \text{ or } A_i - B_i N_i(t) > 0, \\ 0 & \text{otherwise,} \end{cases} \quad (1)$$

where $N_i(t) = \sum_{a \in \mathcal{A}} 1\{s_a(t) = Y_i\}$. Also, A_i, B_i and $R_i(0)$ values are prespecified. The notation $1\{\cdot\}$ represents the indicator function. Therefore, $N_i(t)$ is the number of agents present at target i at time t . According to (1): (i) $R_i(t)$ increases at a rate A_i when no agent is visiting target i , (ii) $R_i(t)$ decreases at a rate $B_i N_i(t) - A_i$ where B_i is the uncertainty removal rate by a visiting agent to the target i , and, (iii) $R_i(t) \geq 0, \forall t$. This problem set-up has an attractive queueing system interpretation [7] where A_i and $B_i N_i(t)$ can be thought of as the arrival rate and the controllable service rate respectively at target (server) $i \in \mathcal{T}$ in a queueing network.

b) Agent Model: Some persistent monitoring models (e.g., [9], [11]) assume each agent $a \in \mathcal{A}$ to have a finite sensing range $r_a > 0$ allowing it to decrease $R_i(t)$ whenever it is in the vicinity of target $i \in \mathcal{T}$ (i.e., when $\|s_a(t) - Y_i\| \leq r_a$). However, this paper follows the approach used in [7], [8] where $r_a = 0$ is assumed and $N_i(t)$ is used to replace the joint detection probability of a target i . Moreover, similar to [8] (see also [12]), the contributions of this paper are invariant to the used dynamic model of the agents.

c) Main Objective: In this problem setup, the main objective is to minimize the measure of *mean system uncertainty* J_T (evaluated over a finite time interval $t \in [0, T]$),

$$J_T \triangleq \frac{1}{T} \int_0^T \sum_{i \in \mathcal{T}} R_i(t) dt, \quad (2)$$

by controlling the motion of the agents.

d) Graph Topology: As the next step, a directed graph topology $\mathcal{G} = (\mathcal{T}, \mathcal{E})$ is embedded into the mission space such that the *targets* are represented by the graph *vertices* ($\mathcal{T} = \{1, 2, \dots, M\}$), and the inter-target *trajectory segments* (that are available for agents to travel between targets) are represented by the graph *edges* ($\mathcal{E} \subseteq \{(i, j) : i, j \in \mathcal{T}\}$). In particular, these trajectory segments may take arbitrary shapes so as to account for potential constraints (for the agent motion) existing in the mission space. It is assumed that each edge $(i, j) \in \mathcal{E}$ has an associated time value $\rho_{ij} \in \mathbb{R}_{\geq 0}$ which represents the amount of time that an agent has to spend to travel from target i to j . The *neighbor set* and the *neighborhood* of a target $i \in \mathcal{T}$ is defined respectively as

$$\mathcal{N}_i \triangleq \{j : (i, j) \in \mathcal{E}\} \text{ and } \tilde{\mathcal{N}}_i = \mathcal{N}_i \cup \{i\}.$$

e) Optimal Solution: Based on this embedded graph topology \mathcal{G} , whenever an agent $a \in \mathcal{A}$ is ready to leave a target $i \in \mathcal{T}$, its *next-visit* would be some target $j \in \mathcal{N}_i$. This implies that the agent will have to use the trajectory segment represented by the edge $(i, j) \in \mathcal{E}$ to arrive at target j - spending a ρ_{ij} amount of time on the process. Subsequently, upon spending some *dwell-time* on target j (which contributes to decrease $R_j(t)$), the agent a will have to make a similar decision again.

Therefore, in this kind of persistent monitoring on graphs (PMG) problems, each agent's trajectory can be fully characterized by the sequence of targets visited and the dwell time spent at each visited target (see also [8]). Hence the optimal method to control the set of deployed agents \mathcal{A} (such that the objective given in (2) is minimized) can be determined in the form of a set of optimal *dwell-time* and *next-visit* decision sequences. However, as pointed out in [7], this is a challenging task even for the simplest PMG problem configurations due to the nature of the search space.

f) Receding Horizon Control: The on-line distributed IPA-TCP method proposed in [7] requires each agent to use a set of *thresholds* applied to its neighborhood target uncertainties $R_j(t)$, $j \in \mathcal{N}_i$ in order to determine its dwell-time and next-visit decisions. Starting from an arbitrary set of thresholds, each agent iteratively adjust these thresholds using a gradient technique that exploits the information

from observed events in agents' trajectories. Although this approach is efficient due to the use of IPA, it is limited by the presence of local optima.

To address this limitation, this paper proposes to use an *Event-Driven Receding Horizon Controller* (ED-RHC) at each agent $i \in \mathcal{T}$. The basic idea of RHC has its root in Model Predictive Control (MPC) but, in addition, it exploits the event-driven nature of the PGM problem to reduce complexity by orders of magnitude and provide flexibility in the frequency of control updates. As introduced in [13] and extended in [10],[14], ED-RHC solve an optimization problem over a given *planning horizon* when an event is observed; the resulting control is then executed over a generally shorter *action horizon* defined by the occurrence of the next event of interest to the controller. This process is iteratively repeated in event-driven fashion. In the PMG problem, the aim of the ED-RHC when invoked at time t with an agent residing at $i \in \mathcal{T}$ is to determine the immediate dwell-time and next-visit decisions, jointly forming a control $U_i(t)$. This is done by solving an optimization problem of the form:

$$U_i^*(t) = \arg \min_{U_i(t) \in \mathbb{U}(t)} [J_H(X_i(t), U_i(t); H) + \hat{J}_H(X_i(t+H))] \quad (3)$$

where $X_i(t)$ is the current local state and $\mathbb{U}(t)$ is the feasible control set at t . The term $J_H(X_i(t), U_i(t); H)$ is the immediate cost over the planning horizon $[t, t+H]$ and \hat{J}_H is an estimate of the future cost evaluated at the end of the planning horizon $t+H$. The value of H is exogenously selected in prior work [13],[15],[14]. However, in this paper we will include this value into the optimization problem and ignore the $\hat{J}_H(X_i(t+H))$ term. Thus, by optimizing the planning horizon we compensate for the inaccuracy of $\hat{J}_H(X_i(t+H))$ in addition to avoiding the complexity of evaluating it. Moreover, note that the proposed ED-RHC is distributed since it allows each agent to separately solve (3) using only local state information.

B. Preliminary Results

According to (1), the uncertainty state profile $R_i(t)$ of a target $i \in \mathcal{T}$ is piece-wise linear and its gradient (i.e., $\dot{R}_i(t)$) changes only when one of the following *events* occur: (i) An agent arrival at i , (ii) An agent departure from i , or when (iii) $R_i(t) \rightarrow 0^+$. Now, take $t = t_i^k$ as the time of occurrence of the k^{th} such event, where, $k \in \mathbb{Z}_{\geq 0}$ and $t_i^0 = 0$. Then,

$$\dot{R}_i(t) = \dot{R}_i(t_i^k), \quad \forall t \in [t_i^k, t_i^{k+1}). \quad (4)$$

Remark 1: Note that if the agents chose to dwell on target i in a *non-overlapping* manner (i.e., one agent at a time), $N_i(t) \in \{0, 1\}$, $\forall t \in [0, T]$ in (1). In such a case, (4) implies that the sequence $\{\dot{R}_i(t_i^k) : k = 0, 1, 2, \dots\}$ is a *cyclic order* of three elements: $\{-(B_i - A_i), 0, A_i\}$.

To make sure that each agent is capable of making $R_i \rightarrow 0^+$ of any $i \in \mathcal{T}$, the following assumption is made in this paper (a more strict assumption have also been used in [8]).

Assumption 1: Target uncertainty rate parameters A_i and B_i of each target $i \in \mathcal{T}$ follow $0 < A_i < B_i$.

Decomposition of the objective function: The following Theorem 1 provides a target-wise and temporal decomposition of the main objective function J_T (in (2)).

Theorem 1: The contribution to the main objective J_T by a target $i \in \mathcal{T}$ during a time period $t \in [t_0, t_1) \subseteq [t_i^k, t_i^{k+1})$ for some $k \in \mathbb{Z}_{\geq 0}$ is $\frac{1}{T} J_i(t_0, t_1)$, where,

$$J_i(t_0, t_1) = \int_{t_0}^{t_1} R_i(t) dt = \frac{(t_1 - t_0)}{2} [2R_i(t_0) + \dot{R}_i(t_0)(t_1 - t_0)]. \quad (5)$$

Proof: In (2), by taking the summation operator out of the integration and then splitting the time interval $t \in [0, T]$ of the integration of $R_i(t)$ profile into three parts gives

$$J_T = \frac{1}{T} \left[\sum_{j \in \mathcal{T} \setminus \{i\}} \int_0^T R_j(t) dt \right] + \frac{1}{T} \left[\int_0^{t_0} R_i(t) dt + \int_{t_0}^{t_1} R_i(t) dt + \int_{t_1}^T R_i(t) dt \right], \quad (6)$$

where \setminus represents the set subtraction operator. Therefore, clearly the contribution of target i to the main objective J_T during the time period $t \in [t_0, t_1)$ is $\frac{1}{T} J_i(t_0, t_1)$ where,

$$J_i(t_0, t_1) = \int_{t_0}^{t_1} R_i(t) dt.$$

Moreover, since $[t_0, t_1) \subseteq [t_i^k, t_i^{k+1})$, the relationship (4) implies that $\int_{t_0}^{t_1} R_i(t) dt$ represents the area of a trapezoid (whose parallel sides are $R_i(t_0)$ and $R_i(t_1)$). Therefore,

$$J_i(t_0, t_1) = \left[\frac{R_i(t_0) + R_i(t_1)}{2} \times (t_1 - t_0) \right].$$

Also, (4) gives that $R_i(t_1) = R_i(t_0) + \dot{R}_i(t_0)(t_1 - t_0)$. Therefore,

$$J_i(t_0, t_1) = \frac{(t_1 - t_0)}{2} [2R_i(t_0) + \dot{R}_i(t_0)(t_1 - t_0)].$$

■

The notation $J_i(t_0, t_1)$ introduced in Theorem 1 will henceforth be used liberally - disregarding the constraint $[t_0, t_1) \subseteq [t_i^k, t_i^{k+1})$ on its arguments t_0 and t_1 . This is because a generic interval $[t_0, t_1)$ can always be decomposed into a finite sequence of inter-event intervals where the Theorem 1 is applicable (for each of those inter-event intervals).

Now, under the scenario described in Remark 2, if a target $i \in \mathcal{T}$ is visited by an agent at $t = t_0$ (take $t_0 = t_i^k$), the subsequent two events (associated with the target i) will be $R_i(t) \rightarrow 0^+$ event (at $t = t_i^{k+1}$) and the agent departure event (at $t = t_i^{k+2}$). Assume t_1 is such that $t_i^{k+2} \leq t_1 < t_i^{k+3}$. The following corollary states the corresponding $J_i(t_0, t_1)$ value.

Corollary 1: For the scenario described above,

$$J_i(t_0, t_1) = \frac{u_i}{2} [2R_i(t_0) - (B_i - A_i)u_i] + \frac{r_i}{2} [A_i r_i],$$

where $u_i = t_i^{k+1} - t_0$, $v_i = t_i^{k+2} - t_i^{k+1}$ and $r_i = t_1 - t_i^{k+2}$.

Proof: Applying Theorem 1 to the three interested inter-event intervals (note that $t_i^k = t_0$) gives

$$J_i(t_0, t_1) = \frac{(t_i^{k+1} - t_0)}{2} [2R_i(t_0) + \dot{R}_i(t_0)(t_i^{k+1} - t_0)] \\ + \frac{(t_i^{k+2} - t_i^{k+1})}{2} [2R_i(t_i^{k+1}) + \dot{R}_i(t_i^{k+1})(t_i^{k+2} - t_i^{k+1})] \\ + \frac{(t_1 - t_i^{k+2})}{2} [2R_i(t_i^{k+2}) + \dot{R}_i(t_i^{k+2})(t_1 - t_i^{k+2})].$$

Now, using: (i) the definitions of u_i, v_i, r_i , (ii) the \dot{R}_i values stated in Remark 2 and (iii) the fact that $R_i(t_i^{k+1}) = R_i(t_i^{k+2}) = 0$, the above expression can be simplified as

$$J_i(t_0, t_1) = \frac{u_i}{2} [2R_i(t_0) - (B_i - A_i)u_i] + \frac{v_i}{2} [2 \cdot 0 + 0 \cdot v_i] \\ + \frac{r_i}{2} [2 \cdot 0 + A_i r_i], \\ = \frac{u_i}{2} [2R_i(t_0) - (B_i - A_i)u_i] + \frac{r_i}{2} [A_i r_i].$$

Local objective function: In a distributed paradigm, it is reasonable to have some *local* information sharing sessions. In this paper, with regard to the considered PMG problem setting, the following interactions are assumed to be local and hence allowed:

- 1) Any target $i \in \mathcal{T}$ receives the information $\{A_j, B_j\}$ at $t = 0$ from its neighbors $j \in \mathcal{N}_i$.
- 2) Any target $i \in \mathcal{T}$ can request for the information $\{R_j(t), \dot{R}_j(t)\}$ at any time t from its neighbors $j \in \mathcal{N}_i$.
- 3) Any agent $a \in \mathcal{A}$ residing in some target $i \in \mathcal{T}$ at a time t (i.e., $s_a(t) = Y_i$) can exploit target i to obtain above two types of information from any $j \in \mathcal{N}_i$.

The *local objective function* of a target i for a time period $t \in [t_0, t_1] \subseteq [0, T]$ is defined as

$$\bar{J}_i(t_0, t_1) = \sum_{j \in \mathcal{N}_i} J_j(t_0, t_1). \quad (7)$$

To evaluate each $J_j(t_0, t_1)$ term involved in the above expression, the time interval $[t_0, t_1]$ first should be broken down into a sequence of corresponding inter-event time intervals. Then, Theorem 1 should be applied (similar to Corollary 1).

Before discussing the proposing ED-RHC solution, the following remark should be made.

Remark 2: As pointed out in [8], multiple agents having overlapping dwell sessions at some target (also known as “target sharing”) is an unfavorable behavior that leads to poor performances. Also, allowing such behaviors complicates the analysis of PMG systems unnecessarily [8]. Therefore, the analysis presented next limits to the cases where no such overlapping dwell sessions occur (at any target). Moreover, the derived ED-RHC solution ensures that such unfavorable behaviors do not occur. Finally, note that this concern does not apply to single-agent PMG problems.

C. Overview to the Event Driven Receding Horizon Control (ED-RHC) Solution

Consider a generic situation where an agent (say $a \in \mathcal{A}$) resides on a certain target (say $i \in \mathcal{T}$). It is assumed

that agent a is made aware of different interesting *local events* occurring in the neighborhood \mathcal{N}_i through local communications (while it resides on i). This is a reasonable assumption to make since the developed ED-RHC solution is a decentralized approach.

In this generic setting, the agent a at some *local event time* $t \in [0, T]$, optimally decides three subsequent decisions that it has to make. They are: (i) the *dwell time* τ_i to remain on the currently residing target i , (ii) the next target $j \in \mathcal{N}_i$ to visit and the *dwell time* τ_j to remain on the visited target j .

A dwell time decision τ_i (or τ_j) can be divided into two inter-dependent decisions: the *active time* u_i (or u_j) and the *inactive time* v_i (or v_j) - as shown in Fig. 1. The time spent to reach the decided next target j is called the *transit time* (i.e., ρ_{ij}). In all, at a local event time t , the agent a has to optimally choose five *decision variables*: u_i, v_i, j, u_j , and v_j .

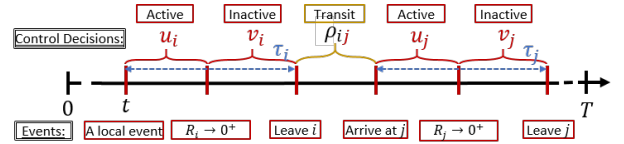


Fig. 1: The control decisions ahead and the event timeline.

Fixed Horizon: A constant $H \in \mathbb{R}$ specified by the user is considered as the *fixed horizon* for the problem of optimally determining the aforementioned decision variables. Since PMG problems only interested in a finite period $[0, T]$, it is reasonable to curb the given H according to the current event time t such that $H := \min\{T - t, H\}$. However, this does not affect the analysis presented next. Hence H is considered as a user-defined constant throughout this paper.

Take the interested continuous decision variables as $U_{ij} = [u_i, v_i, u_j, v_j]$ and the current local state (at t) as $X_i(t) = \{R_j(t) : j \in \mathcal{N}_i\}$. Then, the optimal decision variables are obtained by solving the following set of optimization problems (henceforth called as the ED-RHC Problem (RHCP)):

$$U_{ij}^* = \arg \min_{U_{ij} \in \mathbb{U}} J_H(X_i(t), U_{ij}; H); \quad \forall j \in \mathcal{N}_i, \text{ and,} \quad (8)$$

$$j^* = \arg \min_{j \in \mathcal{N}_i} J_H(X_i(t), U_{ij}^*; H). \quad (9)$$

Note that (8) involves solving $|\mathcal{N}_i|$ number of optimization problems and (9) is only a numerical comparison. Therefore, the final optimal decision variables are: U_{ij}^* and j^* . Here, the notation $|\cdot|$ denotes the 1-norm or the cardinality operator when the argument is a matrix or a set, respectively.

The conventional choices for the *RHC objective function* J_H and the *feasible control space* \mathbb{U} of the RHCP are

$$J_H(X_i(t), U_{ij}; H) = \frac{1}{H} \bar{J}_i(t, t+H), \text{ and,} \\ \mathbb{U} = \{U : U \in \mathbb{R}^4, U \geq 0, |U| + \rho_{ij} = H\}. \quad (10)$$

This RHC objective function choice (10) is intuitive as it forces the agent a to choose its decision variables so as to minimize the average contribution to J_T in (2) from the neighborhood \mathcal{N}_i - over the given fixed horizon H (i.e., over

the period $[t, t+H]$). Moreover, the equality constraint in the \mathbb{U} in (10) can simplify the evaluation of (8).

However, the use of (10) in RHCP is problematic as it can result in agent behaviors that are heavily dependent on the choice of H . For example, if H is very large (or very small), clearly the optimal decisions given by U_{ij}^* and j^* are sub-optimal. Attempting to find the optimal choice of H without compromising the on-line distributed nature of the solution is a challenging task.

Variable Horizon: To address this problem, a concept named *variable horizon* (denoted by w) is introduced where,

$$w \triangleq |U_{ij}| + \rho_{ij} = u_i + v_i + \rho_{ij} + u_j + v_j. \quad (11)$$

In fact, w can be thought of as an auxiliary variable that depends on the decision variables. Now, the RHC objective function J_H and the feasible control space \mathbb{U} in the RHCP are chosen as

$$J_H(X_i(t), U_{ij}; H) = \frac{1}{w} \bar{J}_i(t, t+w), \text{ and,} \\ \mathbb{U} = \{U : U \in \mathbb{R}^4, U \geq 0, |U| + \rho_{ij} \leq H\}. \quad (12)$$

Note that having the constraint $|U_{ij}| + \rho_{ij} \leq H$ ensures $w \leq H$. Hence (12) encompasses all the feasible control decisions covered by (10). Thus, the performance will only improve by adopting (12). Moreover, having a variability in the used horizon metric (i.e., w) in (12) enables simultaneous determination of the *optimum horizon size*: $w^* = |U_{ij}^*| + \rho_{ij}^*$.

On the other hand, having a variable denominator term in the RHC objective and having one extra dimension in the feasible control space are two challenges that need to be addressed to use (12). For this purpose, different structural properties of (12) are exploited in this paper and it is shown that (8) in this case can be solved analytically and efficiently (note that (8) is the non-trivial problem out of (8) and (9)). Intricate details on how the RHCP (with (12)) is solved are provided in the remaining sections of this paper.

Action Horizon: Recall that, when agent a resides in target i , upon any local event, it needs to solve the RHCP to determine the optimal decision variables: U_{ij}^* and j^* . The agent a follows these optimal decisions only until some other local event is observed (at some time after t). This time period in-between locally observed events where an agent adheres to its (pre)determined optimal trajectory is called the action horizon and denoted by h . Fig. 2 shows how three subsequent action horizons observed (labeled h_1, h_2 and h_3) after the initial local event occurred at t . Note that w_1, w_2 and w_3 in Fig. 2 represents the three optimum horizon sizes (i.e., w^* values) determined at each respective local event time: t , $t+h_1$ and $t+h_1+h_2$.

Since the action horizon h is determined by the events happening in the neighborhood, agent a does not have any control over it. However, h can be upper-bounded as each optimal decision variable defines a subsequent (local) event time. To illustrate this point, consider the following example (see also Fig. 3).

- If $u_{i,t}^*$ represents the optimum active to be spent at i determined at the local event time t , then, the action horizon

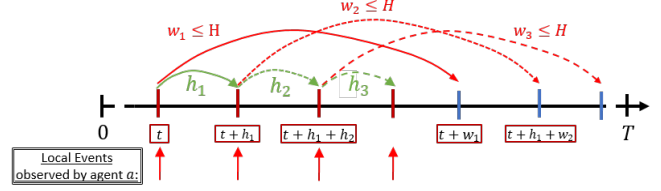


Fig. 2: Event driven receding horizon control approach.

(say h_1) follows: $h_1 \leq u_{i,t}^*$. This is because if no other local event is observed during $[t, t+u_{i,t}^*]$, at $t = t+u_{i,t}^*$ the event: $R_i \rightarrow 0^+$ will occur (see Fig. 1).

- In such a case, $h_1 = u_{i,t}^*$ and the agent a will re-evaluate the RHCP at $t+h_1$. Now, the RHCP should only consider determining the optimal decisions: v_i, j, u_j and v_j (simpler than before). Hence, the subsequent action horizon (say h_2) is bounded as: $h_2 \leq v_{i,t+h_1}^*$, because if no other local event is observed during $[t+h_1, t+h_1+v_{i,t+h_1}^*]$, at $t+h_1+v_{i,t+h_1}^*$ the event: agent leaving target i will occur.

- If things further continued in a similar manner (having only *strictly local* events), $h_2 = v_{i,t+h_1}^*$, and at $t+h_1+h_2$, the RHCP should be re-evaluated again. However, now the aim should be to determine the optimal decisions: j, u_j and v_j (simplest). Therefore, if the subsequent action horizon is h_3 , it is directly $h_3 = \rho_{im}$ where $m = j_{t+h_1+h_2}^*$, which is the optimally decided next-visit target at $t+h_1+h_2$. Now, note that at $t+h_1+h_2+h_3$, the agent a will arrive at (new) target m triggering a local event in the (new) neighborhood \mathcal{N}_m .

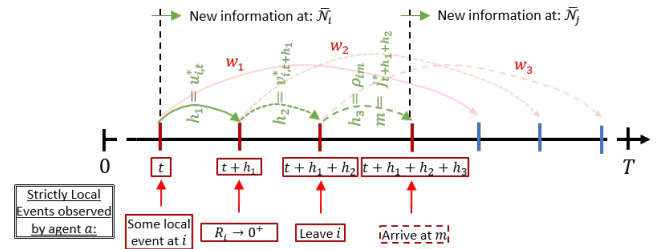


Fig. 3: Agent a 's action horizons when it faces strictly local events (i.e., events occurred on the residing target).

Three variants of the RHCP: From the above example, apart from the fact that the action horizon h being bounded, it should be also clear that there are three variants of the RHCP depending on when it is evaluated. In this paper, when required, quantities belonging to a specific variant is identified using a superscript l where $l \in \{1, 2, 3\}$. For example, the RHCP^l is aimed at determining optimal decisions of: U_{ij}^l and j where

$$U_{ij}^1 = [u_i, v_i, u_j, v_j], \quad U_{ij}^2 = [v_i, u_j, v_j], \quad U_{ij}^3 = [u_j, v_j].$$

Precisely, the RHCP^l is

$$U_{ij}^{l*} = \arg \min_{U_{ij}^l \in \mathbb{U}^l} J_H^l(X_i(t), U_{ij}^l; H); \quad \forall j \in \mathcal{N}_i, \\ j^* = \arg \min_{j \in \mathcal{N}_i} J_H^l(X_i(t), U_{ij}^{l*}; H), \quad (13)$$

where $w^{(l)} \triangleq |U_{ij}^l| + \rho_{ij}$ and

$$J_H^l(X_i(t), U_{ij}^l; H) = \frac{1}{w^{(l)}} \bar{J}_i(t, t + w^{(l)}),$$

$$\mathbb{U}^l = \{U : U \in \mathbb{R}^{5-l}, U \geq 0, |U| + \rho_{ij} \leq H\}. \quad (14)$$

The next three sections of this paper are dedicated to present the solutions (with their properties) of each RHCP variant. However, before going into that, few minor concerns need to be addressed concerning multi-agent scenarios.

D. Handling the presence of multiple agents

Maintaining non-overlapping dwell sessions at each target: As pointed out in Remark 2, in multi-agent scenarios, agents should avoid dwelling in the same target simultaneously. In the proposed ED-RHC approach, this can be ensured by introducing a small modification.

A target $j \in \mathcal{T}$ is said to be *covered* at time t if it already has a residing agent or if an agent is en route to visit it from a neighboring target in \mathcal{N}_j . The notation $\mathcal{C}(t)$ is used to represent the set of all the covered targets at time t . In other words, a target $j \in \mathcal{C}(t)$ only if $\exists k \in \mathcal{N}_j$ and $\tau \in [t, t + \rho_{kj})$, such that

$$\sum_{a \in \mathcal{A}} 1\{s_a(\tau) = Y_j\} > 0.$$

Under a paradigm where neighboring targets communicate with each other, this condition (i.e., whether $j \in \mathcal{C}(t)$) can be determined at any target j at any time t .

Now, an agent $a \in \mathcal{A}$ residing in a target i (as shown in Fig. 1) can prevent having an overlapping dwell time at target $j \in \mathcal{N}_i$ in the future by simply modifying the notion of the neighbor set \mathcal{N}_i used in the RHCP (evaluated at t) such that

$$\mathcal{N}_i := \mathcal{N}_i \setminus \mathcal{C}(t). \quad (15)$$

The appropriateness of this technique is evident from the RHCP³ where its immediate choice directs the agent a to travel to the optimum neighbor $j^* \in \mathcal{N}_i$. Therefore, having $j^* \notin \mathcal{C}(t)$ is important and is guaranteed by (15). Note that as soon as agent a becomes en route to j^* , j^* becomes covered (preventing any other agent from visiting j^* prior to agent a 's subsequent departure from j^*).

Computing \bar{J}_i : The existence of multiple agents hinders the ability to analytically express the function $\bar{J}_i(t, t + w)$ involved in the RHCP as it requires the agent a (whom is residing in i at t planning a trajectory that visits neighbor j) to have the knowledge of the events that will occur at each neighbor $m \in \mathcal{N}_i \setminus \{j\}$ during the future time period $[t, t + w)$ (see (12), (7) and Theorem 1).

However, this task becomes tractable when the aforementioned neighbor-set modification in (15) is employed. For example, upon using (15), if some neighbor $m \in \mathcal{N}_i \setminus \{j\}$, then, there is no other agent residing in or en route to target m at t . Therefore, clearly, $\dot{R}_m(\tau) = A_m$ for the period $\tau \in [t, t + r)$ where $r \geq \min_{q \in \mathcal{N}_m} \rho_{qm}$. Now, if $[t, t + r) \subseteq [t, t + w)$, projections are used to estimate the remaining portion of the $R_m(\tau)$ profile (i.e. for $\tau \in [t + r, t + w]$). This enables expressing $\bar{J}_i(t, t + w)$ analytically.

Local Events: In the light of the modification and approximation techniques discussed above for the multi-agent scenarios (based on the “covered” nature of the neighbors), this is a good point to revisit and to provide a precise definition of the term *local events*.

Consider the generic agent a whom is residing in target i at time t . Viable *strictly local events* to agent a and the respective RHCP variant that needs to be evaluated are as follows:

- 1) Agent a 's arrival at i if at time t . \implies RHCP¹,
- 2) $h = u_{i,t}^*$ with $R_i(t + h) > 0$ at time $t + h$. \implies RHCP³
- 3) $R_i(t + \tau) \rightarrow 0^+$ at $t + \tau$. \implies RHCP²
- 4) $h = v_{i,t}^*$ with $R_i(t) = 0$ at time $t + h$. \implies RHCP³

Similarly, viable *neighbor induced local events* to agent a (by the neighbor $j \in \mathcal{N}_i$) are as follows:

- 1) Target j become uncovered at some time $t + \tau \geq t$.
- 2) Target j become covered at some time $t + \tau \geq t$.

Note that, upon observing either of the above two events, the agent a should evaluate: RHCP¹ if $R_i(t + \tau) > 0$ or RHCP² if $R_i(t + \tau) = 0$.

It is expected that each agent re-evaluating its RHCP at these different types of local events observed in their trajectories can improve the global performance in an efficient manner, while also compensating for any sub-optimality stemming from the aforementioned modification (15) and the approximation. This concludes the overview of the proposed ED-RHC solution.

III. SOLVING THE EVENT-DRIVEN RECEDING HORIZON CONTROL PROBLEM VARIANT - 3 (RHCP³)

An agent $a \in \mathcal{A}$ residing in target i at some local event time t has to evaluate the RHCP³ when it is ready to leave i . Therefore, the RHCP³ involves only three decision variables: j and $U_{ij}^3 = [u_j, v_j]$ (as u_i, v_i decisions are irrelevant in this case). Out of these three decision variables, the obtained optimum choice for $j = j^*$ is directly taken as the next destination to visit. Thus, the RHCP³ plays a crucial role in defining each agent's trajectory.

As shown in Fig. 1, upon leaving target i at time t , the agent a plans to visit neighbor target j and spend an active time of u_j and an inactive time of v_j on j . The variable horizon (i.e., w in (11)) for this case is defined as $w^{(3)} \triangleq \rho_{ij} + u_j + v_j$. According to the feasible control space definition in (12), $w^{(3)}$ should be constrained so that $\rho_{ij} \leq w^{(3)} \leq H$ where H is the known fixed horizon. Therefore, targets $j \in \mathcal{N}_i$ where $\rho_{ij} > H$ are omitted from evaluating (8) of the RHCP³. Thus, $\rho_{ij} \leq H$ is assumed henceforth in this section.

1. Constraints: As mentioned in Section II-C, the decision variables u_j and v_j are inter-dependent due to the nature of the target uncertainty dynamics (1). Specifically, any dynamically feasible decision pair (u_j, v_j) should belong to one of the two classes defined below:

$$\begin{cases} \text{Class 1: } 0 \leq u_j \leq \lambda_{j0} \text{ and } v_j = 0, \text{ or,} \\ \text{Class 2: } u_j = \lambda_{j0} \text{ and } v_j > 0 \end{cases} \quad (16)$$

where λ_{j0} is the maximum active time possible to spend on target j - which will make $R_j \rightarrow 0$ under the given initial conditions. Using (1), λ_{j0} can be written as

$$\lambda_{j0} = \frac{R_j(t + \rho_{ij})}{B_j - A_j} = \frac{R_j(t) + A_j \rho_{ij}}{B_j - A_j}. \quad (17)$$

Note that λ_{j0} is a constant that only depends on: initial target uncertainty $R_j(t)$, target parameters A_j, B_j , and transit time ρ_{ij} . Moreover, note the fact that in order to spend a non zero inactive time (i.e., $v_j > 0$), the agent has to first spend the maximum active time possible (i.e., $u_j = \lambda_{j0}$).

Now, the above two classes are redefined to incorporate the horizon constraint: $w^{(3)} = |U_{ij}^3| + \rho_{ij} \leq H$ as follows.

$$\begin{cases} \text{Class 1: } 0 \leq u_j \leq \lambda_j \text{ and } v_j = 0, \text{ or,} \\ \text{Class 2: } u_j = \lambda_{j0} \text{ and } 0 < v_j \leq \mu_j, \end{cases} \quad (18)$$

where λ_{j0} is given in (17) and

$$\begin{aligned} \lambda_j &\triangleq \min\{\lambda_{j0}, H - \rho_{ij}\}, \text{ and,} \\ \mu_j &\triangleq H - (\rho_{ij} + \lambda_{j0}). \end{aligned}$$

Here, λ_j and μ_j represent the maximum possible u_j and v_j values respectively. Now, any decision $U_{ij}^3 = [u_j, v_j]$ that follows (18) is feasible for the RHCP³, i.e., $U_{ij}^3 \in \mathbb{U}^3$ where

$$\mathbb{U}^3 = \{U : U \geq 0, U \in \mathbb{R}^2, |U| + \rho_{ij} \leq H\} \text{ (from (12)).}$$

2. Objective: According to the generic RHCP objective function definition given in (12), the objective function corresponding to the RHCP³ is taken as $J_H^3(U_{ij}^3)$ where

$$J_H^3(U_{ij}^3) = J_H(X_i(t), [0, 0, U_{ij}^3]; H) = \frac{1}{w^{(3)}} \bar{J}_i(t, t + w^{(3)}).$$

To obtain an expression for J_H^3 , first, the local objective function \bar{J}_i is decomposed as (using (7))

$$\bar{J}_i = J_j + \sum_{m \in \mathcal{N}_i \setminus \{j\}} J_m. \quad (19)$$

Now, considering the case where agent a goes from target i to target j following decisions u_j and v_j as shown in Fig. 4, both J_j and J_m terms in (19) are evaluated for the period $[t, t + w^{(3)})$ using Theorem 1. This gives

$$\begin{aligned} J_j &= \frac{\rho_{ij}}{T} [2R_j(t) + A_j \rho_{ij}] + \frac{u_j}{T} [2(R_j(t) + A_j \rho_{ij}) \\ &\quad - (B_j - A_j)u_j], \text{ and} \\ J_m &= \frac{(\rho_{ij} + u_j + v_j)}{T} [2R_m(t) + A_m(\rho_{ij} + u_j + v_j)]. \end{aligned}$$

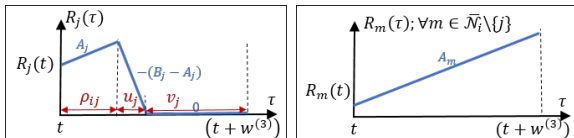


Fig. 4: State trajectories of targets in \mathcal{N}_i during $[t, t + w^{(3)})$

Now, combining the above two results and substituting it in (19) gives the complete objective function $J_H^3(U_{ij}^3)$ as

$$J_H^3(u_j, v_j) = \frac{C_1 u_j^2 + C_2 v_j^2 + C_3 u_j v_j + C_4 u_j + C_5 v_j + C_6}{\rho_{ij} + u_j + v_j}, \quad (20)$$

where,

$$\begin{aligned} C_1 &= \frac{1}{2} [\bar{A} - B_j], \quad C_2 = \frac{\bar{A}_j}{2}, \quad C_3 = \bar{A}_j, \\ C_4 &= [\bar{R}(t) + \bar{A} \rho_{ij}], \quad C_5 = [\bar{R}_j(t) + \bar{A}_j \rho_{ij}], \\ C_6 &= \frac{\rho_{ij}}{2} [2\bar{R}(t) + \bar{A} \rho_{ij}], \end{aligned}$$

and (the neighborhood parameters)

$$\begin{aligned} \bar{A}_{ij} &= \sum_{m \in \mathcal{N}_i \setminus \{j\}} A_m, \quad \bar{R}_{ij}(t) = \sum_{m \in \mathcal{N}_i \setminus \{j\}} R_m(t), \\ \bar{A}_i &= \bar{A}_{ij} + A_j, \quad \bar{A}_j = \bar{A}_{ij} + A_i, \quad \bar{A} = \bar{A}_{ij} + A_i + A_j, \\ \bar{R}_i &= \bar{R}_{ij} + R_j, \quad \bar{R}_j = \bar{R}_{ij} + R_i, \quad \bar{R} = \bar{R}_{ij} + R_i + R_j. \end{aligned} \quad (21)$$

Note that all the coefficients stated above are non-negative except for C_1 which is non-negative only when: $B_j \leq \bar{A}$.

3. Solving the RHCP³ for optimal control (u_j^*, v_j^*): Based on the first step of RHCP (8), (u_j^*, v_j^*) is given by

$$\begin{aligned} (u_j^*, v_j^*) &= \arg \min_{(u_j, v_j)} J_H^3(u_j, v_j) \\ (u_j, v_j) &\text{ s.t. (18).} \end{aligned} \quad (22)$$

- **Class 1:** First, assume (u_j^*, v_j^*) belongs to the Class 1 defined in (18). Then, $v_j = v_j^* = 0$ and (22) takes the form:

$$\begin{aligned} u_j^* &= \arg \min_{u_j} J_H^3(u_j, 0) \\ 0 &\leq u_j < \lambda_j. \end{aligned} \quad (23)$$

where λ_j is given in (18).

Lemma 1: The optimal solution for (23) is

$$u_j^* = \begin{cases} \lambda_j & \text{if } \lambda_j \geq u_j^\# \text{ and } \bar{A} < B_j, \\ 0 & \text{otherwise,} \end{cases} \quad (24)$$

where $u_j^\#$ is

$$u_j^\# = \frac{\bar{A} \rho_{ij}}{B_j - \bar{A}}. \quad (25)$$

Proof: Using (20), first and second order derivatives of $J_H^3(u_j, 0)$ can be obtained respectively as $J'(u_j)$ and $J''(u_j)$,

$$J'(u_j) = \frac{\bar{A} - B_j}{2} + \frac{B_j \rho_{ij}^2}{2(\rho_{ij} + u_j)^2}, \quad J''(u_j) = -\frac{B_j \rho_{ij}^2}{(\rho_{ij} + u_j)^3}.$$

Notice that $J'(0) > 0$ and $J''(u_j) < 0, \forall u_j > 0$. This implies that $J'(u_j)$ is monotonically decreasing with $u_j > 0$. Also note that $\lim_{u_j \rightarrow \infty} J'(u_j) = \frac{\bar{A} - B_j}{2}$.

Therefore, for the case where $\bar{A} \geq B_j$, the objective $J_H^3(u_j, 0)$ is monotonically increasing with u_j . Hence $u_j^* = 0$ in (23).

For the case where $\bar{A} < B_j$, the limiting value of $J'(u_j)$ is negative. This implies an existence of a maximum (of $J_H^3(u_j, 0)$) at some $u_j > 0$. However, such a maximizing u_j value is irrelevant to (23). Nevertheless, a crucial u_j value is

located at the point where $J_H^3(0,0) = J_H^3(u_j,0)$ occurs. Using (20), this can be determined as $u_j = \frac{C_6 - C_4 \rho_{ij}}{C_1}$ which simplifies to $u_j = u_j^\#$ where $u_j^\#$ is given in (25).

According to the nature of $J'(u_j)$ and $J''(u_j)$, it is clear that $J_H^3(u_j,0)$ should be decreasing with $u_j \geq u_j^\#$ (below $J_H^3(0,0)$ value). Therefore, when $\lambda_j \geq u_j^\#$ (and $\bar{A} < B_j$), $u_j^* = \lambda_j$ in (23). ■

Note that $u_j^\#$ in (25) can be thought of as a break-even point for u_j , where when λ_j allows u_j to go beyond such a $u_j^\#$ value, it is always optimal to do so by choosing $u_j = \lambda_j$.

Remark 3: When H is sufficiently large, according to (18) and (17), $\lambda_j = \lambda_{j0} = \frac{R_j(t) + A_j \rho_{ij}}{B_j - A_j}$. Therefore, the condition $\lambda_j \geq u_j^\#$ used in (23) becomes state dependent (specifically on $R_j(t)$). For a such case, u^* in (23) becomes

$$u_j^* = \begin{cases} \lambda_j & \text{if } R_j(t) \geq \rho_{ij} \left[\frac{B_j - A_j}{B_j - \bar{A}} \cdot \bar{A} - A_j \right] \text{ and } \bar{A} < B_j, \\ 0 & \text{otherwise.} \end{cases} \quad (26)$$

- Class 2: Now, assume (u_j^*, v_j^*) belongs to the Class 2 defined in (18). Then, $u_j = u_j^* = \lambda_{j0}$ and (22) takes the form:

$$v_j^* = \arg \min_{v_j} J_H^3(\lambda_{j0}, v_j) \quad (27)$$

$$0 < v_j \leq \mu_j$$

Lemma 2: The optimal solution for (27) is

$$v_j^* = \begin{cases} 0^+ & \text{if } \bar{A} \geq B_j \left[1 - \frac{\rho_{ij}^2}{(\rho_{ij} + \lambda_{j0})^2} \right] \\ v_j^\# & \text{else if } v_j^\# \leq \mu_j \\ \mu_j & \text{otherwise,} \end{cases} \quad (28)$$

where 0^+ is a positive constant that is arbitrarily closer to 0 and $v_j^\#$ is

$$v_j^\# = \sqrt{\frac{(B_j - A_j)(\rho_{ij} + \lambda_{j0})^2 - B_j \rho_{ij}^2}{\bar{A}_j}} - (\rho_{ij} + \lambda_{j0}). \quad (29)$$

Proof: Similar to the proof of Lemma 1, using (20), first and second order derivatives of $J_H^3(\lambda_{j0}, v_j)$ with respect to v_j can be obtained respectively as $J'(v_j)$ and $J''(v_j)$, where

$$J'(0) = \frac{\bar{A}}{2} - \frac{B_j}{2} \left[1 - \frac{\rho_{ij}^2}{(\rho_{ij} + \lambda_{j0})^2} \right],$$

$$J''(v_j) = \frac{R_j^2(t) + 2B_j \rho_{ij} R_j(t) + A_j B_j \rho_{ij}^2}{(B_j - A_j)(\rho_{ij} + \lambda_{j0} + v_j)}.$$

Note that $J''(v_j) > 0$ for all $v_j \geq 0$. This implies that $J_H^3(\lambda_{j0}, v_j)$ is convex in the positive orthant of v_j , and $J'(v_j)$ is increasing with $v_j > 0$ starting from $J'(0)$ given above.

Now, if $J'(0) \geq 0$, it implies that $J_H^3(\lambda_{j0}, v_j)$ is monotonically increasing with $v_j > 0$. Therefore, for such a case, $v_j^* = 0^+$ and it proves the first case in (28).

When $J'(0) < 0$, there should exist a minimum to $J_H^3(\lambda_{j0}, v_j)$ at some $v_j > 0$. Using calculus, the minimizing v_j value can be found easily as $v_j = v_j^\#$ given in (29).

Now, based on the constraint $0 < v_j \leq \mu_j$ in (28) and the convexity of $J_H^3(\lambda_{j0}, v_j)$, it is clear that whenever $v_j^\# \leq \mu_j \implies$

$v_j^* = v_j^\#$ in (28) and whenever $v_j^\# > \mu_j \implies v_j^* = \mu_j$. This proves the last two cases given in (28). ■

Unlike $u_j^\#$ given in (25) for the problem (23), $v_j^\#$ given in (29) for the problem (27) is an optimal choice available for v_j . Therefore, whenever the constraints on v_j (i.e., $0 < v_j \leq \mu_j$) allow choosing $v_j = v_j^\#$, it should be executed.

Remark 4: The terms λ_{j0} and μ_j involved in (28) can be simplified (using (17) and (18) respectively) to illustrate the state dependent nature of v_j^* as

$$v_j^* = \begin{cases} 0^+ & \text{if } \bar{A} \geq B_j \text{ or } R_j(t) \leq \left[\frac{\rho_{ij}(B_j - A_j)\sqrt{B_j}}{\sqrt{B_j - \bar{A}}} - \rho_{ij} B_j \right] \\ v_j^\# & \text{else if } R_j(t) \leq \left[\sqrt{(B_j - A_j)(H^2 \bar{A}_j + \rho_{ij} B_j)} - \rho_{ij} B_j \right] \\ \mu_j & \text{otherwise.} \end{cases} \quad (30)$$

- Combined Result:

Theorem 2: The optimal solution of (22) is

$$(u_j^*, v_j^*) = \begin{cases} (0, 0) & \text{if } u_j^\# > \lambda_j \text{ or } \bar{A} \geq B_j \\ (\lambda_j, 0) & \text{else if } \lambda_j < \lambda_{j0} \\ (\lambda_{j0}, 0) & \text{else if } B_j > \bar{A} \geq B_j \left[1 - \frac{\rho_{ij}^2}{(\rho_{ij} + \lambda_{j0})^2} \right] \\ (\lambda_{j0}, v_j^\#) & \text{else if } v_j^\# \leq \mu_j \\ (\lambda_{j0}, \mu_j) & \text{otherwise,} \end{cases} \quad (31)$$

where $u_j^\#$ is given in (25) and $v_j^\#$ is given in (29).

Proof: This result is a composition of the respective solutions given in Lemma 1 and 2 for the optimization problems (23) and (27). ■

Based on the cases where the first condition in (31) is not satisfied, the following remark can be made.

Remark 5: The above theorem implies that whenever: (i) the fixed time horizon H is sufficiently large, (ii) the sensing capabilities are higher $B_j > \bar{A}$ and (iii) target uncertainty $R_j(t)$ is larger than some known threshold, it is optimum to plan ahead to empty the target j 's uncertainty upon visiting it (i.e., $u_j^* = \lambda_{j0}$). This conclusion is inline with the Theorem 1 proposed in [7].

4. Solving for optimum next destination j^* : Using Theorem 2, when the agent a is ready to leave target i at some local event time t , it can compute the optimal trajectory costs $J_H^3(u_j^*, v_j^*)$ for all $j \in \mathcal{N}_i$. Note that $J_H^3(u_j^*, v_j^*)$ is heavily dependent on $\{R_j(t), \lambda_j, \mu_j, A_j, B_j, \rho_{ij}\}$ values.

Having such a dependence is crucial. Appendix B provides a counter example where the same RHCP³ have been considered but with a different objective function form (other than (12)). For that case, it is proven that (see Theorem 4 and (70)) $J_H^3(u_j^*, v_j^*)$ is dependent only on ρ_{ij} - which leads to unfavorable results (see Theorem 5).

Based on the second step of the RHCP (i.e., (9)), the optimum neighbor to visit next is j^* where

$$j^* = \arg \min_{j \in \mathcal{N}_i} J_H^3(u_j^*, v_j^*). \quad (32)$$

In the case of RHCP³, as shown in Fig. 2, above j^* in (32) defines the "Action" that the agent has to take at (current)

time t . In other words, the agent a has to leave target i at time t and follow the path $(i, j^*) \in \mathcal{E}$ to visit target j^* .

Remark 6: When constructing the objective function of the RHCP³, instead of using the local objective function decomposition given in (19), using a weighted version of it such as

$$\bar{J}_i = \alpha J_j + (1 - \alpha) \sum_{m \in \mathcal{N}_i \setminus \{j\}} J_m \quad (33)$$

for some fixed $\alpha \in [0, 1]$ is a feasible choice which have been found to be more effective in some numerical examples. An ED-RHC approach where this modified RHCP³ objective function is used is labeled as ED-RHC ^{α} . Also, it should be noted that this modification does not cause any non-trivial changes to the presented theoretical results.

IV. SOLVING THE EVENT-DRIVEN RECEDING HORIZON CONTROL PROBLEM VARIANT - 2 (RHCP²)

As described in Section II, an agent $a \in \mathcal{A}$ residing in target i at some local event time t has to evaluate the RHCP² only if the occurred event is: (i) a strictly local $R_i \rightarrow 0^+$ event, or (ii) a neighbor induced event while $R_i(t) = 0$. Therefore, the decision variable u_i of the original RHCP formulation is irrelevant for this case. Hence the RHCP² involves only four decision variables: $U_{ij}^2 = [v_i, u_j, v_j]$ and j . Out of these four, the optimum choice for $v_i = v_i^*$ is taken as the inactive time ahead to be spent at target i - prior to leaving (unless any neighbor induced event occurs).

As shown in Fig. 1, the agent plans to spend an inactive time of v_i on i (starting from the current time t) and then to visit neighbor j to spend an active time of u_j and an inactive time of v_j on j . The variable horizon (i.e., w in (11)) for this case is defined as $w^{(2)} \triangleq v_i + \rho_{ij} + u_j + v_j$. Similar to the case with RHCP³ discussed in the previous section, targets $j \in \mathcal{N}_i$ where $\rho_{ij} > H$ are omitted from evaluating (8) of the RHCP² and $\rho_{ij} \leq H$ is assumed.

1. Constraints: Similar to before, u_j and v_j are inter-dependent due to the target j 's uncertainty dynamics (1). Therefore, they follow the physical constraints given in (16). Similarly, target i 's uncertainty dynamics (1) constrain $v_i \geq 0$.

Recall that λ_{j0} in (16) (i.e., (17)) is the required active time to make $R_j \rightarrow 0$. However, due to the inclusion of v_i , now, λ_{j0} is dependent on v_i . Therefore, this section uses the notation $\lambda_{j0} = \lambda_{j0}(v_i)$ where, (using (1), redefining (17))

$$\lambda_{j0}(v_i) = \frac{R_j(t + v_i + \rho_{ij})}{B_j - A_j} = \frac{R_j(t) + A_j \rho_{ij}}{B_j - A_j} + \frac{A_j}{B_j - A_j} \cdot v_i \quad (34)$$

As it will be shown next, the other control limiting parameters (i.e., μ_i, λ_j and μ_j) now become control dependent (i.e., either on v_i, u_j or v_j).

Now, the physical constraints in (16) are developed to incorporate (34) and the horizon constraints (i.e., $w^{(2)} \leq H$) stated above. This defines two classes for feasible $[v_i, u_j, v_j]$ values for the RHCP² as follows:

$$\begin{aligned} &0 \leq v_i \leq \mu_i(u_j, v_j) \text{ and} \\ &\begin{cases} \text{Class 1: } 0 \leq u_j \leq \lambda_j(v_i) \text{ and } v_j = 0, \\ \text{Class 2: } u_j = \lambda_{j0}(v_i) \text{ and } 0 < v_j \leq \mu_j(v_i), \end{cases} \end{aligned} \quad (35)$$

where, $\lambda_{j0}(v_i)$ is given in (34) and

$$\begin{aligned} \mu_i(u_j, v_j) &= H - (\rho_{ij} + u_j + v_j), \\ \lambda_j(v_i) &= \min\{\lambda_{j0}(v_i), H - (v_i + \rho_{ij})\}, \\ \mu_j(v_i) &= H - (v_i + \rho_{ij} + \lambda_{j0}(v_i)). \end{aligned}$$

Similar to (18), λ_j and μ_j respectively represent the limiting values of active and inactive times at j . Along the same lines, μ_i is the upper bound to the inactive time at i . However, in contrast to (18), the aforementioned three quantities are control dependent in (35).

Moreover, note that in (35), under Class 1, $\mu_i(u_j, v_j) = \mu_i(u_j, 0)$ and under Class 2, $\mu_i(u_j, v_j) = \mu_i(\lambda_{j0}(v_i), v_j)$. Now, any decision $U_{ij}^2 = [v_i, u_j, v_j]$ that follows (35) is feasible for the RHCP², i.e., $U_{ij}^2 \in \mathbb{U}^2$ where

$$\mathbb{U}^2 = \{U : U \geq 0, U \in \mathbb{R}^3, |U| + \rho_{ij} \leq H\} \quad (\text{from (12)}).$$

2. Objective: Following from the generic RHCP objective function definition in (12), the objective function corresponding to the RHCP² is taken as $J_H^2(U_{ij}^2)$ where

$$J_H^2(U_{ij}^2) = J_H(X_i(t), [0, U_{ij}^2]; H) = \frac{1}{w^{(2)}} \bar{J}_i(t, t + w^{(2)}).$$

In order to obtain an expression for J_H^2 , \bar{J}_i in (7) is decomposed as,

$$\bar{J}_i = J_i + J_j + \sum_{m \in \mathcal{N}_i \setminus \{j\}} J_m. \quad (36)$$

Now, each of the above three terms J_i, J_j and J_m should be evaluated for a case where agent a goes from target i to j following the decisions v_i, u_j, v_j during the period $[t, t + w^{(2)}]$. State trajectories for a such situation are shown in Fig. 5. Similar to before, Theorem 1 is utilized for this purpose which gives:

$$\begin{aligned} J_i &= \frac{A_i(\rho_{ij} + u_j + v_j)^2}{2}, \\ J_j &= \frac{(v_i + \rho_{ij})}{2} [2R_j(t) + A_j(v_i + \rho_{ij})] \\ &\quad + \frac{u_j}{2} [2(R_j(t) + A_j(v_i + \rho_{ij})) - (B_j - A_j)u_j], \\ J_m &= \frac{(v_i + \rho_{ij} + u_j + v_j)}{2} [2R_m(t) + A_m(v_i + \rho_{ij} + u_j + v_j)]. \end{aligned}$$

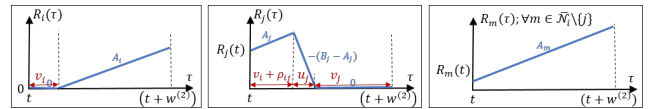


Fig. 5: State trajectories of targets in \mathcal{N}_i during $[t, t + w^{(2)}]$

Now, combining the above three results and substituting it in (36) gives the complete objective function $J_H^2(U_{ij}^2)$ as

$$J_H^2(v_i, u_j, v_j) = \frac{[C_1 v_i^2 + C_2 u_j^2 + C_3 v_j^2 + C_4 v_i u_j + C_5 v_i v_j + C_6 u_j v_j + C_7 v_i + C_8 u_j + C_9 v_j + C_{10}]}{v_i + \rho_{ij} + u_j + v_j}, \quad (37)$$

where

$$\begin{aligned} C_1 &= \frac{\bar{A}_i}{2}, \quad C_2 = \frac{\bar{A} - B_j}{2}, \quad C_3 = \frac{\bar{A}_j}{2}, \quad C_4 = \bar{A}_i, \quad C_5 = \bar{A}_{ij}, \\ C_6 &= \bar{A}_j, \quad C_7 = [\bar{R}_i(t) + \bar{A}_i \rho_{ij}], \quad C_8 = [\bar{R}_i(t) + \bar{A} \rho_{ij}], \\ C_9 &= [\bar{R}_{ij}(t) + \bar{A}_j \rho_{ij}] \text{ and } C_{10} = \frac{\rho_{ij}}{2} [2\bar{R}_i(t) + \bar{A} \rho_{ij}]. \end{aligned}$$

The remaining parameters are same as (21). Note that all the coefficients stated above are non-negative except for C_2 , where $C_2 \geq 0 \iff \bar{A} \geq B_j$.

3. Solving the RHCP² for optimal control (v_i^*, u_j^*, v_j^*)

: Based on the first step of the generic RHCP given in (8), the optimal controls for the RHCP² are determined by

$$\begin{aligned} (v_i^*, u_j^*, v_j^*) &= \arg \min_{(v_i, u_j, v_j)} J_H^2(v_i, u_j, v_j) \\ (v_i, u_j, v_j) &\text{ s.t. (35).} \end{aligned} \quad (38)$$

- **Class 1:** First assume (v_i^*, u_j^*, v_j^*) belongs to the Class 1 defined in (35). Then, $v_j = v_j^* = 0$ and (38) takes the form:

$$\begin{aligned} (v_i^*, u_j^*) &= \arg \min_{(v_i, u_j)} J_H^2(v_i, u_j, 0) \\ v_i &\geq 0, \\ 0 &\leq u_j < \lambda_{j0}(v_i), \\ v_i + u_j &< H - \rho_{ij}. \end{aligned} \quad (39)$$

The above constraints are a result of the constraints in (35) and the relationships:

$$\begin{aligned} v_i &\leq \mu_i(u_j, 0) \iff v_i \leq H - (\rho_{ij} + u_j), \text{ and,} \\ u_j &< \lambda_j(v_i) \iff u_j < \lambda_{j0}(v_i) \ \& \ u_j < H - (v_i + \rho_{ij}). \end{aligned}$$

Note that $\lambda_{j0}(v_i)$ is linear in v_i (see (34)).

- **Class 2:** Now, assume (v_i^*, u_j^*, v_j^*) belongs to the Class 2 defined in (35). Then, $u_j = u_j^* = \lambda_{j0}(v_i^*)$ and (38) takes the form:

$$\begin{aligned} (v_i^*, v_j^*) &= \arg \min_{(v_i, v_j)} J_H^2(v_i, \lambda_{j0}(v_i), v_j) \\ v_i &\geq 0, \\ v_j &> 0, \\ v_i + \lambda_{j0}(v_i) + v_j &\leq H - \rho_{ij}. \end{aligned} \quad (40)$$

The last constraint in (40) is a result of (35) and the relationships:

$$\begin{aligned} v_i &\leq \mu_i(\lambda_{j0}(v_i), v_j) \iff v_i \leq H - (\rho_{ij} + \lambda_{j0}(v_i) + v_j), \text{ and,} \\ v_j &\leq \mu_j(v_i) \iff v_j \leq H - (v_i + \rho_{ij} + \lambda_{j0}(v_i)). \end{aligned}$$

- **Combined Result:** The formulated optimization problems (39) and (40) (even also (22)) directly belongs to the class of *constrained rational function optimization problems* (RFOPs) discussed in Appendix A (see (59)). Specifically, Appendix A presents a computationally cheap theoretical solution developed for such RFOPs.

Upon individually obtaining solutions to (39) and (40), the main optimization problem (38) is solved by just comparing objective function values of individual solutions.

4. Solving for optimal (planned) next destination j^* :

The second step of the RHCP² (similar to (9)) is to choose the optimum neighbor j according to

$$j^* = \arg \min_{j \in \mathcal{N}_i} J_H^2(v_i^*, u_j^*, v_j^*). \quad (41)$$

Note that this step requires the cost value of the optimal solution $U_{ij}^{2*} = [v_i^*, u_j^*, v_j^*]$ obtained for each $j \in \mathcal{N}_i$ (in (38)). Now, v_i^* taken from U_{ij}^{2*} defines the ‘‘Action’’ that the agent has to take at current time t . In other words, such v_i^* is the inactive time that the agent should spend on current target i starting from the current time t before leaving.

V. SOLVING THE EVENT-DRIVEN RECEDING HORIZON CONTROL PROBLEM VARIANT - 1 (RHCP¹)

An agent $a \in \mathcal{A}$ residing in target i at some local event time t has to evaluate the RHCP¹ only if the occurred event is: (i) the agent a 's own arrival at i , or (ii) a neighbor induced event while $R_i(t) > 0$. Therefore, all the decision variables (i.e., $U_{ij}^1 = [u_i, v_i, u_j, v_j]$ and j) of the original RHCP formulation is relevant for this case. Out of these five decisions, the optimum choice for $u_i = u_i^*$ is implemented directly as the active time ahead to be spent at target i - until the next local event occurs.

As shown in Fig. 1, starting from current time t the agent plans to spend active and inactive times first at target i (u_i and v_i respectively) and then at target j (u_j and v_j respectively). The variable horizon (i.e., w in (11)) for this case is defined as $w^{(1)} \triangleq u_i + v_i + \rho_{ij} + u_j + v_j$. Similar to the RHCP² and RHCP³ discussed before, targets $j \in \mathcal{N}_i$ where $\rho_{ij} > H$ are omitted from evaluating (8) of the RHCP¹ and thus $\rho_{ij} \leq H$ is assumed in the following formulation.

1. Constraints: The physical constraints given in (16) are now applied to both targets i and j . In there, λ_{i0} and λ_{j0} are respectively used to represent the sensing times required to make $R_i \rightarrow 0$ and $R_j \rightarrow 0$. While both λ_{i0} and λ_{j0} are dependent on the respective initial conditions, target parameters and transit time, λ_{j0} has an extra dependence on the control decisions u_i and v_i . Hence the notation $\lambda_{j0} = \lambda_{j0}(u_i, v_i)$ is used in this section. Explicitly, (using (1))

$$\begin{aligned} \lambda_{i0} &= \frac{R_i(t)}{B_i - A_i}, \text{ and} \\ \lambda_{j0} &= \lambda_{j0}(u_i, v_i) = \frac{R_j(t) + A_j \rho_{ij}}{B_j - A_j} + \frac{A_j}{B_j - A_j} \cdot (u_i + v_i). \end{aligned} \quad (42)$$

Now, the physical constraints in (16) are developed to incorporate (42) and the horizon constraints (i.e., $w^{(1)} \leq H$) stated above. This defines four classes named as Class 1A, 1B, 2A and 2B for feasible $[u_i, v_i, u_j, v_j]$ values for the RHCP¹ as follows:

$$\left\{ \begin{array}{l} \text{Class 1: } 0 \leq u_i < \lambda_i(u_j, v_j) \text{ and } v_i = 0, \\ \text{Class 2: } u_i = \lambda_{i0} \text{ and } 0 < v_i \leq \mu_i(u_j, v_j), \end{array} \right\} \times \left\{ \begin{array}{l} \text{Class A: } 0 \leq u_j < \lambda_j(u_i, v_i) \text{ and } v_j = 0, \\ \text{Class B: } u_j = \lambda_{j0}(u_i, v_i) \text{ and } 0 < v_j \leq \mu_j(u_i, v_i), \end{array} \right\} \quad (43)$$

where, λ_{i0} and $\lambda_{j0}(u_i, v_i)$ are given in (42) and

$$\begin{aligned}\lambda_i(u_j, v_j) &= \min\{\lambda_{i0}, H - (\rho_{ij} + u_j + v_j)\}, \\ \mu_i(u_j, v_j) &= H - (\lambda_{i0} + \rho_{ij} + u_j + v_j), \\ \lambda_j(u_i, v_i) &= \min\{\lambda_{j0}(u_i, v_i), H - (u_i + v_i + \rho_{ij})\}, \\ \mu_j(u_i, v_i) &= H - (u_i + v_i + \rho_{ij} + \lambda_{j0}(u_i, v_i)).\end{aligned}$$

Similar to (18) and (35), the notation λ_j and μ_j respectively represent the limiting values of active and inactive times feasible at j . And λ_i and μ_i represent the same for target i . However, unlike in (18) or (35), each of these four limiting values are now dependent on two control decisions. Now, any decision $U_{ij}^1 = [u_i, v_i, u_j, v_j]$ that belongs to one of the classes in (43), is feasible for the RHCP¹, i.e., $U_{ij}^1 \in \mathbb{U}^1$ where

$$\mathbb{U}^1 = \{U : U \geq 0, U \in \mathbb{R}^4, |U| + \rho_{ij} \leq H\} \text{ (from (12))}$$

2. Objective: According to the RHCP objective function given in (12), that of RHCP¹ is taken as $J_H^1(U_{ij}^1)$ where

$$J_H^1(U_{ij}^1) = J_H(X_i(t), U_{ij}^1; H) = \frac{1}{w^{(1)}} \bar{J}_i(t, t + w^{(1)}).$$

To obtain an expression for $J_H^1(U_{ij}^1)$, \bar{J}_i (defined in (7)) is decomposed as (36). Next, the three terms J_i , J_j and J_m are evaluated for a case where the agent goes from target i to j following decisions U_{ij}^1 during the period $[t, t + w^{(1)}]$. State trajectories for a such scenario is given in Fig. 6. Theorem 1 is utilized for this purpose to obtain:

$$\begin{aligned}J_i &= \frac{u_i}{2} [2R_i(t) - (B_i - A_i)u_i] + \frac{(\rho_{ij} + u_j + v_j)}{2} \\ &\quad \times [2(R_i(t) - (B_i - A_i)u_i) + A_i(\rho_{ij} + u_j + v_j)], \\ J_j &= \frac{(u_i + v_i + \rho_{ij})}{2} [2R_j(t) + A_j(u_i + v_i + \rho_{ij})] \\ &\quad + \frac{u_j}{2} [2(R_j(t) + A_j(u_i + v_i + \rho_{ij})) - (B_j - A_j)u_j], \\ J_m &= \frac{(u_i + v_i + \rho_{ij} + u_j + v_j)}{2} [2R_m(t) \\ &\quad + A_m(u_i + v_i + \rho_{ij} + u_j + v_j)].\end{aligned}$$

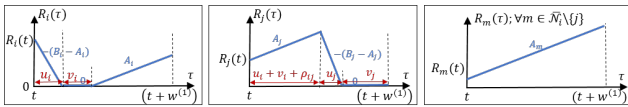


Fig. 6: State trajectories of targets in \mathcal{N}_i during $[t, t + w^{(1)}]$

Now, combining the above three results and substituting it in (36) gives the complete objective function $J_H^1(U_{ij}^1)$ as

$$J_H^1(u_i, v_i, u_j, v_j) = \frac{\begin{aligned} &C_1 u_i^2 + C_2 v_i^2 + C_3 u_j^2 + C_4 v_j^2 + C_5 u_i v_i \\ &+ C_6 u_i u_j + C_7 u_i v_j + C_8 v_i u_j + C_9 v_i v_j + C_{10} u_j v_j \\ &+ C_{11} u_i + C_{12} v_i + C_{13} u_j + C_{14} v_j + C_{15} \end{aligned}}{u_i + v_i + \rho_{ij} + u_j + v_j}, \quad (44)$$

where

$$\begin{aligned}C_1 &= \frac{\bar{A} - B_i}{2}, \quad C_2 = \frac{\bar{A}_i}{2}, \quad C_3 = \frac{\bar{A} - B_j}{2}, \quad C_4 = \frac{\bar{A}_j}{2}, \\ C_5 &= \bar{A}_i, \quad C_6 = \bar{A} - B_i, \quad C_7 = \bar{A}_j - B_i, \quad C_8 = \bar{A}_i, \\ C_9 &= \bar{A}_{ij}, \quad C_{10} = \bar{A}_j, \quad C_{11} = [\bar{R}(t) + (\bar{A} - B_i)\rho_{ij}], \\ C_{12} &= [\bar{R}_i(t) + \bar{A}_i \rho_{ij}], \quad C_{13} = [\bar{R}(t) + \bar{A} \rho_{ij}], \\ C_{14} &= [\bar{R}_j(t) + \bar{A}_j \rho_{ij}] \quad \text{and} \quad C_{15} = \frac{\rho_{ij}}{2} [2\bar{R}(t) + \bar{A} \rho_{ij}].\end{aligned}$$

The remaining parameters are same as (21). Note that all the coefficients stated above are non-negative except for C_1, C_3, C_6, C_7 and C_{11} .

3. Solving the RHCP¹ for optimal control ($u_i^*, v_i^*, u_j^*, v_j^*$): The first step of the RHCP¹ can be stated based on (8) and (44) as:

$$\begin{aligned}(u_i^*, v_i^*, u_j^*, v_j^*) &= \arg \min_{(u_i, v_i, u_j, v_j)} J_H^1(u_i, v_i, u_j, v_j) \\ &\quad (u_i, v_i, u_j, v_j) \text{ s.t. (43)}.\end{aligned} \quad (45)$$

- Class 1A: First assume $(u_i^*, v_i^*, u_j^*, v_j^*)$ belongs to the Class 1A defined in (43). Then, $v_i = v_i^* = 0$, $v_j = v_j^* = 0$ and (45) takes the form:

$$\begin{aligned}(u_i^*, u_j^*) &= \arg \min_{(u_i, u_j)} J_H^1(u_i, 0, u_j, 0) \\ &\quad 0 \leq u_i < \lambda_{i0}, \\ &\quad 0 \leq u_j < \lambda_{j0}(u_i, 0), \\ &\quad u_i + u_j < H - \rho_{ij}.\end{aligned} \quad (46)$$

To write the constraints in (46), (43) and the relationships:

$$\begin{aligned}u_i < \lambda_i(u_j, 0) &\iff u_i < \lambda_{i0} \text{ \& } u_i < H - (\rho_{ij} + u_j), \text{ and,} \\ u_j < \lambda_j(u_i, 0) &\iff u_j < \lambda_{j0}(u_i, 0) \text{ \& } u_j < H - (u_i + \rho_{ij}),\end{aligned}$$

have been used. Note that $\lambda_{j0}(u_i, 0)$ is linear and increasing with u_i (see (42)).

- Class 1B: Now assume $(u_i^*, v_i^*, u_j^*, v_j^*)$ belongs to the Class 1B defined in (43). Then, $v_i = v_i^* = 0$, $u_j = u_j^* = \lambda_{j0}(u_i^*, 0)$ and (45) takes the form:

$$\begin{aligned}(u_i^*, v_j^*) &= \arg \min_{(u_i, v_j)} J_H^1(u_i, 0, \lambda_{j0}(u_i, 0), v_j) \\ &\quad 0 \leq u_i < \lambda_{i0}, \\ &\quad v_j > 0, \\ &\quad u_i + \lambda_{j0}(u_i, 0) + v_j \leq H - \rho_{ij}.\end{aligned} \quad (47)$$

The constraints in (47) are from (43) and the relationships:

$$\begin{aligned}u_i < \lambda_i(\lambda_{j0}(u_i, 0), v_j) &\iff \\ u_i < \lambda_{i0} \text{ \& } u_i < H - (\rho_{ij} + \lambda_{j0}(u_i, 0) + v_j), \text{ and,} \\ v_j < \mu_j(u_i, 0) &\iff v_j \leq H - (u_i + \rho_{ij} + \lambda_{j0}(u_i, 0)).\end{aligned}$$

- Class 2A: Now assume $(u_i^*, v_i^*, u_j^*, v_j^*)$ belongs to the Class 2A defined in (43). Then, $u_i = u_i^* = \lambda_{i0}$, $v_j = v_j^* = 0$ and (45) takes the form:

$$\begin{aligned}(v_i^*, u_j^*) &= \arg \min_{(v_i, u_j)} J_H^1(\lambda_{i0}, v_i, u_j, 0) \\ &\quad v_i > 0, \\ &\quad 0 \leq u_j < \lambda_{j0}(\lambda_{i0}, v_i), \\ &\quad v_i + u_j \leq H - (\lambda_{i0} + \rho_{ij}).\end{aligned} \quad (48)$$

The constraints in (48), are from (43) and the relationships:

$$\begin{aligned} v_i &\leq \mu_i(u_j, 0) \iff v_i \leq H - (\lambda_{i0} + \rho_{ij} + u_j), \text{ and,} \\ u_j &< \lambda_j(\lambda_{i0}, v_i) \iff \\ u_j &< \lambda_{j0}(\lambda_{i0}, v_i) \ \& \ u_j < H - (\lambda_{i0} + v_i + \rho_{ij}). \end{aligned}$$

Note that $\lambda_{j0}(\lambda_{i0}, v_i)$ is linear and increasing with v_i (42).

- **Class 2B:** Now, assume $(u_i^*, v_i^*, u_j^*, v_j^*)$ belongs to the Class 2B defined in (43). Then, $u_i = u_i^* = \lambda_{i0}$, $u_j = u_j^* = \lambda_{j0}(\lambda_{i0}, v_i^*)$, and (38) takes the form:

$$\begin{aligned} (v_i^*, v_j^*) &= \arg \min_{(v_i, v_j)} J_H^1(\lambda_{i0}, v_i, \lambda_{j0}(\lambda_{i0}, v_i), v_j) \\ v_i &> 0, \\ v_j &> 0, \\ v_i + v_j + \lambda_{j0}(\lambda_{i0}, v_i) &\leq H - (\lambda_{i0} + \rho_{ij}). \end{aligned} \quad (49)$$

To write the last constraint in (49), (43) and the relationships:

$$\begin{aligned} v_i &\leq \mu_i(\lambda_{j0}(\lambda_{i0}, v_i), v_j) \iff \\ v_i &\leq H - (\lambda_{i0} + \rho_{ij} + \lambda_{j0}(\lambda_{i0}, v_i) + v_j), \text{ and,} \\ v_j &\leq \mu_j(\lambda_{i0}, v_i) \iff v_j \leq H - (\lambda_{i0} + v_i + \rho_{ij} + \lambda_{j0}(\lambda_{i0}, v_i)), \end{aligned}$$

have been used.

- **Combined Result:** The optimization problems (46), (47), (48) and (49) formulated above belong to the class of constrained rational function optimization problems (59) discussed in Appendix A (similar to (39), (40) and (22)). Therefore, each of these four problems are solved exploiting the computationally cheap theoretical solution presented in Appendix B.

Upon obtaining solutions to (46)-(49), the main optimization problem (45) is solved by just comparing objective function values of the obtained individual solutions.

4. Solving for optimal (planned) next destination j^* :

The second step of the RHCP¹ (same as (9)) is to choose the optimum neighbor j according to

$$j^* = \arg \min_{j \in \mathcal{N}_i} J_H^1(u_i^*, v_i^*, u_j^*, v_j^*). \quad (50)$$

Note that this step requires the cost value of the optimal solution $U_{ij}^{1*} = \{u_i^*, v_i^*, u_j^*, v_j^*\}$ obtained for each $j \in \mathcal{N}_i$ (in (45)). As shown in Fig. 2, u_i^* chosen from U_{ij}^{1*} defines the ‘‘Action’’ that the agent has to take at $t = t$. In other words, such u_i^* (depends on j^*) is the active time that the agent should spend on current target i - until the next local event occurs.

VI. SIMULATION RESULTS

This section compares the performance (i.e., J_T in (2)) obtained for several different persistent monitoring problem configurations using: (i) the proposed event-driven receding horizon control (ED-RHC) method, (ii) the RD-RHC ^{α} method suggested in Remark 6, and (iii) the infinitesimal perturbation analysis based threshold control policy (IPA-TCP) method proposed in [7]. Note that all three methods: ED-RHC, ED-RHC ^{α} and IPA-TCP solutions are on-line and distributed (in contrast to the off-line and centralized solution proposed in [8]). All three of these solutions have been

implemented in a JavaScript based simulator, which is made available at <http://www.bu.edu/codes/simulations/shiran27/PersistentMonitoring/>. Readers are invited to reproduce the reported results and also to try new problem configurations using the developed interactive simulator.

Specifically, this section considers the four single-agent problem configurations shown in Figs. 8-11 and the four multi-agent problem configurations shown in Fig. 12-15. In each problem configuration diagram, blue circles represent the targets, while black lines represent available path segments that agents can take to travel between targets. Red triangles and the yellow vertical bars indicate the agent locations and the target uncertainty levels, respectively. Moreover, since both of those quantities are time-varying (i.e., $s_a(t)$ and $R_i(t)$), in figures, their state at the terminal time $t = T$ is shown (upon using either ED-RHC or IPA-TCP solution in the simulation).

In each problem configuration, the used problem parameters are as follows. The target parameters were chosen as $A_i = 1$, $B_i = 10$ and $R_i(0) = 0.5$, $\forall i \in \mathcal{T}$. Also, the used target location co-ordinates (i.e., Y_i) are specified in each problem configuration figure. Note that in all the examples, all the targets have been placed inside a 600×600 mission space. The interested time period was taken as $T = 500$. Each agent’s maximum speed was taken as 50 units per second. The initial locations of the agents were chosen such that they are uniformly distributed among the targets at $t = 0$ (i.e., $s_a(0) = Y_i$ with $i = 1 + (a - 1) * \text{round}(M/N)$). The time horizon H was chosen as $H = 250$ for the two ED-RHC approaches and $\alpha = 0.05$ was used for the ED-RHC ^{α} .

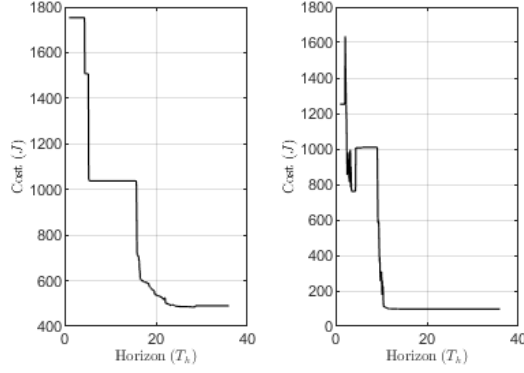
Each sub-figure caption (in Figs. 8-15) provides the cost value (i.e., J_T in (2)) observed under the used controller (i.e., either ED-RHC, ED-RHC ^{α} or IPA-TCP). These cost values are summarized in Tab. I. For the problem configurations shown in Fig. 11 and 15, the respective sub-figures in Fig. 7 shows the performance of the ED-RHC solution (i.e., J_T) under different different time horizon values (i.e., H). In each case, the optimum time horizon value and its corresponding (minimum) cost value are indicated in the respective sub-figure caption.

From Tab. I, note that the proposed ED-RHC method has performed considerably better (on average 50.4% better) than the IPA-TCP method for multi-agent problem configurations. Also, for single-agent problem configurations, both methods have performed equally. The proposed ED-RHC ^{α} approach (in Remark 6) further improves these performances compared to the IPA-TCP method: on average by 67.2% for multi-agent situations and by 2.76% for single agent situations. It is also worth pointing out that the IPA-TCP method has an on-line gradient-based parameter tuning process. Hence the proposed ED-RHC method is far more robust and computationally cheap.

Cost vs. time horizon plots shown in 7 implies that having a large enough time horizon can directly give a performance level that is very closer to the optimum (within 1.1%). Hence, there is no evident importance of attempting to fine-tune the H value. Moreover, note that the complexity of the ED-RHC

TABLE I: Summary of obtained results across all the simulation examples.

J_T in (2)	Single Agent Simulation Examples				Multi-Agent Simulation Examples			
	1	2	3	4	1	2	3	4
IPA-TCP	22.9	47.1	129.2	497.9	270.2	91.7	274.0	201.3
ED-RHC	22.4	47.1	141.4	490.4	105.5	63.7	114.1	97.2
ED-RHC $^\alpha$	22.9	47.1	121.4	473.2	95.4	39.0	63.6	60.3



(a) SASE 4
Min Cost: $J_T = 484.1$ at
Horizon: $H = 12.27$.

(b) MASE 4
Min Cost: $J_T = 96.1$ at
Horizon: $H = 12.27$.

Fig. 7: Cost J_T vs horizon H plot for SASE4 and MASE4.

solution is invariant to the H value.

VII. CONCLUSION

This paper considers the optimal multi-agent persistent monitoring problem defined on a set of targets interconnected according to a fixed graph topology. In order to develop an on-line distributed solution to such PMG problems, departing from existing computationally expensive and slow threshold-based parametric control solutions, a novel computationally cheap and robust event-driven receding horizon control solution is proposed. Specifically, the discrete-event nature of the PMG systems is exploited to determine locally optimum trajectory decisions for each agent to make at different discrete event times on their trajectory. Numerical results obtained from this ED-RHC method show significant improvements compared to the existing parametric control solutions. Ongoing work is aimed to combine desirable features of parametric control strategies and the proposed ED-RHC approach so as to construct a dynamic and (locally) optimal parametric control solution to the PMG problem.

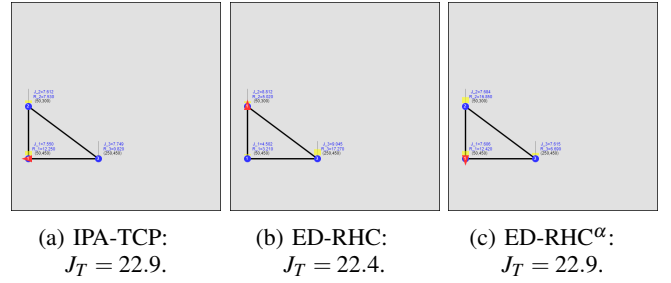


Fig. 8: Single-agent simulation example 1 (SASE1) with 3 targets (state shown at terminal time $t = T$).

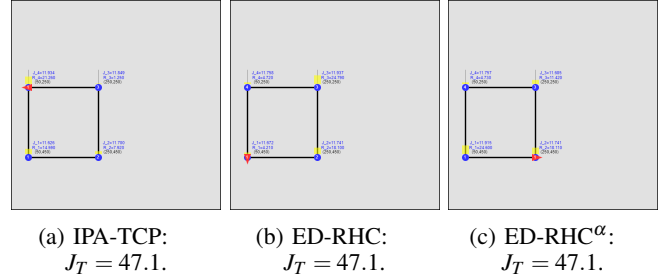


Fig. 9: Single-agent simulation example 2 (SASE2) with 4 targets (state shown at terminal time $t = T$).

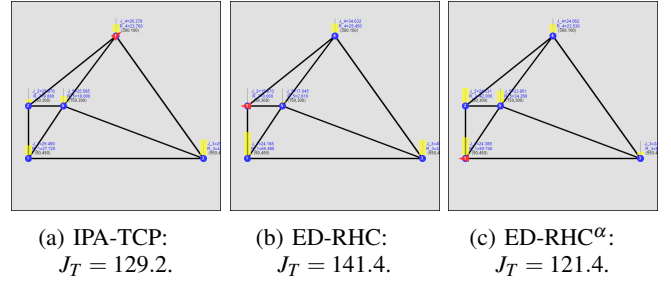


Fig. 10: Single-agent simulation example 3 (SASE3) with 5 targets (state shown at terminal time $t = T$).

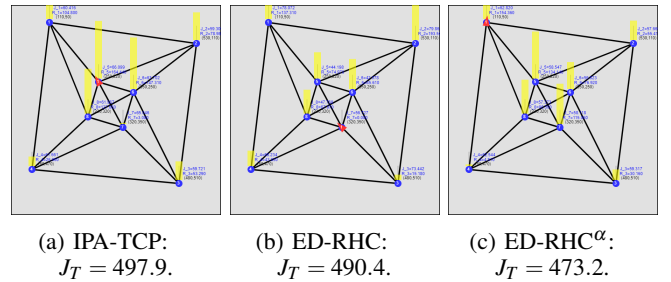


Fig. 11: Single-agent simulation example 4 (SASE4) with 8 targets (state shown at terminal time $t = T$).

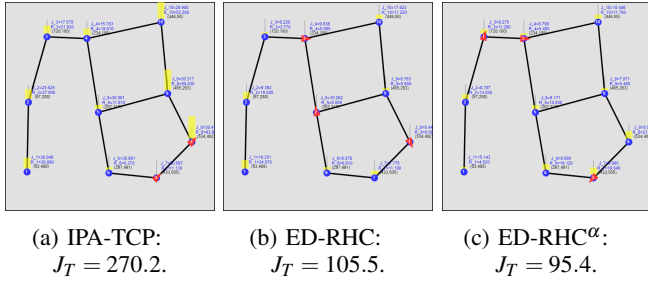


Fig. 12: Multi-agent simulation example 1 (MASE1) with 3 agents and 9 targets (state shown at terminal time $t = T$).

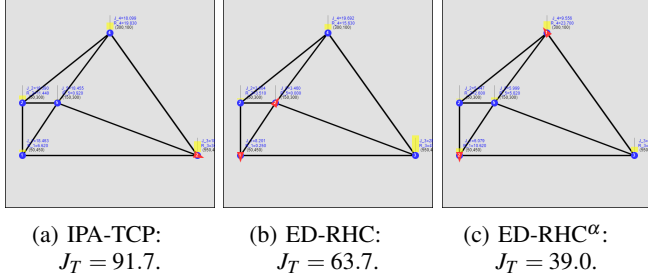


Fig. 13: Multi-agent simulation example 2 (MASE2) with 2 agents and 5 targets (state shown at terminal time $t = T$).

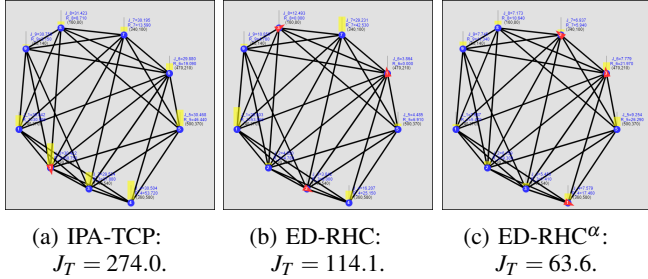


Fig. 14: Multi-agent simulation example 3 (MASE3) with 3 agents and 9 targets (state shown at terminal time $t = T$).

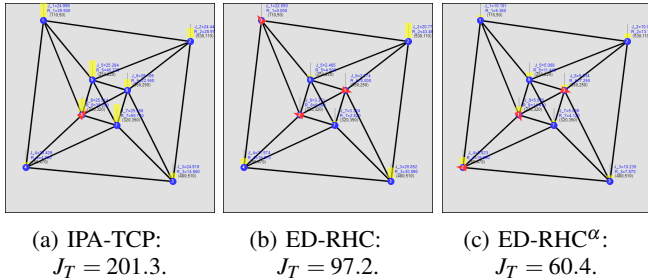


Fig. 15: Multi-agent simulation example 4 (MASE4) with 3 agents and 8 targets (state shown at terminal time $t = T$).

APPENDIX

A. Constrained optimization of bivariate rational functions

1. Convexity of rational functions: Consider a rational function $h: \mathbb{R} \rightarrow \mathbb{R}$ of the form $h(r) = \frac{f(r)}{g(r)}$ and assume $g(r) > 0, \forall r \in \mathcal{U} \subseteq \mathbb{R}$ where \mathcal{U} is a closed interval. In the following discussion, when writing $f(r), g(r)$ or $h(r)$, their argument

is omitted for notational convenience. Also, the notation “ $'$ ” is used to denote the derivative of a function with respect to r .

Lemma 3: Whenever $g(r)$ and $f(r)$ polynomials satisfy

$$g[gf''' - fg'''] - 3g''[gf' - fg'] = 0, \forall r \in \mathcal{U}, \quad (51)$$

$h(r)$ is convex (or concave) on \mathcal{U} if $\Delta_h(r_0) > 0$ (or $\Delta_h(r_0) < 0$) where $r_0 \in \mathcal{U}$ and

$$\Delta_h(r) \triangleq g[gf'' - fg''] - 2g'[gf' - fg']. \quad (52)$$

Proof: The first and second order derivatives of $h(r)$ can be written respectively as

$$h' = \frac{gf' - fg'}{g^2} \text{ and } h'' = \frac{g[gf'' - fg''] - 2g'[gf' - fg']}{g^3}.$$

Note that $h''(r) = \frac{\Delta_h(r)}{g^3(r)}$ and $g^3(r) > 0, \forall r \in \mathcal{U}$. Therefore, convexity of $h(r)$ will only depend on the condition:

$$h''(r) > 0, \forall r \in \mathcal{U} \iff \Delta_h(r) > 0, \forall r \in \mathcal{U}.$$

This condition is easily satisfied whenever

$$\Delta_h(r_0) > 0 \text{ for some } r_0 \in \mathcal{U} \text{ and } \Delta_h'(r) = 0 \text{ for all } r \in \mathcal{U}.$$

Finally, deriving $\Delta_h'(r)$ which yields the expression in (51)

$$\Delta_h'(r) = g[gf''' - fg'''] - 3g''[gf' - fg']$$

completes the proof. \blacksquare

Remark 7: The condition given in (51) (in Lemma 3) is a sufficient condition for the convexity (or concavity) of $h(r)$ on \mathcal{U} . As an example, it is satisfied whenever the denominator polynomial $g(r)$ is of first degree and the numerator polynomial $f(r)$ is of second degree.

2. Constrained minimization of $h(r)$: Assume $h(r)$ to be a rational function which satisfies the conditions discussed above: $g(r) > 0, \Delta_h'(r) = 0, \forall r \in \mathcal{U} \subseteq \mathbb{R}$. Further, assume the signs of $\Delta_h(r_0)$ and $h'(r_0)$ are known at some point of interest $r = r_0 \in \mathcal{U}$ (recall that the sign of $\Delta_h(r_0)$ mimics the sign of $h''(r), r \in \mathcal{U}$). According to Lemma 3, the latter assumption fully determines the convexity (or concavity) of $h(r)$ on \mathcal{U} and its gradient direction at $r = r_0$, respectively. Now, consider the following optimization problem:

$$\begin{aligned} r^* &= \underset{r}{\operatorname{argmin}} h(r) \\ r_0 &\leq r \leq r_1, \end{aligned} \quad (53)$$

where the constrained interval: $[r_0, r_1] \subseteq \mathcal{U}$. A critical r value $r = r^\#$ (which is important to the analysis) is defined as

$$r^\# \triangleq \begin{cases} \{r: h'(r) = 0, r > r_0\} & \text{if } \Delta_h(r_0) > 0 \text{ \& } h'(r_0) < 0, \\ \{r: h(r) = h(r_0), r > r_0\} & \text{if } \Delta_h(r_0) < 0 \text{ \& } h'(r_0) > 0. \end{cases} \quad (54)$$

Note that the two cases considered above are the only cases where a stationary point of $h(r)$ could occur for some $r > r_0, r \in \mathcal{U}$ (see also Fig. 16).

Lemma 4: The optimal solution to (53) is as follows:

If $\Delta_h(r_0) < 0$ & $h'(r_0) > 0$

$$r^* = \begin{cases} r_1 & \text{if } r_1 > r^\#, \\ r_0 & \text{otherwise,} \end{cases}$$

else if $\Delta_h(r_0) > 0$ & $h'(r_0) < 0$,

$$r^* = \begin{cases} r^\# & \text{if } r_1 > r^\#, \\ r_1 & \text{otherwise,} \end{cases}$$

otherwise,

$$r^* = \begin{cases} r_0 & \text{if } \Delta_h(r_0) \geq 0 \text{ \& } h'(r_0) \geq 0, \\ r_1 & \text{otherwise.} \end{cases}$$

Proof: The proof is supported by the Fig. 16. ■

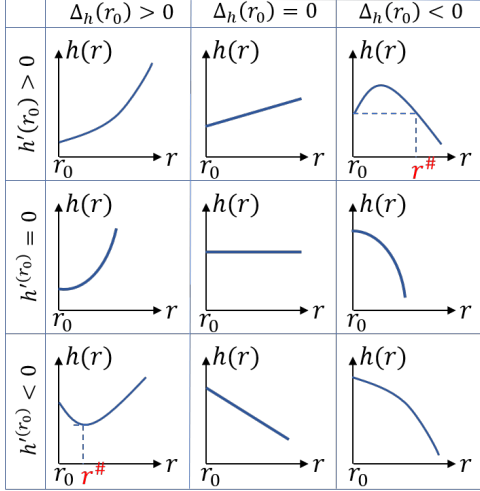


Fig. 16: Graphs of possible $\{h(r) : r \geq r_0, r \in \mathcal{U}\}$ profiles for different cases of $h'(r_0)$ and $\Delta_h(r_0)$ (recall $\text{sgn}(\Delta_h(r_0)) = \text{sgn}(h''(r))$ determines the convexity or concavity).

In essence, an optimization problem of the form (53) can be solved purely based on the numerical values: $h'(r_0)$, $\Delta_h(r_0)$ and $r^\#$. Note that $r^\#$ is only required in two special cases and for the application example mentioned in Remark 7, it can be obtained simply by solving for the roots of a quadratic expression (single variable).

3. Bivariate rational functions: Next, consider the class of *bivariate rational functions* that can be represented by a function $H : \mathbb{R}_+^2 \rightarrow \mathbb{R}$ of the form

$$H(x,y) = \frac{F(x,y)}{G(x,y)} = \frac{C_1x^2 + C_2y^2 + C_3xy + C_4x + C_5y + C_6}{C_7x + C_8y + C_9}, \quad (55)$$

where the coefficients (i.e., $C_1, C_2, C_3, C_4, C_5, C_6, C_7, C_8, C_9$) are known scalar constants with $C_7 \geq 0$, $C_8 \geq 0$ and $C_9 > 0$. Note that the range space of $H(x,y)$ is limited to the non-negative orthant of \mathbb{R}^2 (denoted by \mathbb{R}_+^2).

Developing conditions for the convexity of $H(x,y)$ is complex. Even if such conditions were derived, interpreting them and exploiting them to solve a two dimensional constrained optimization problem that involves minimizing $H(x,y)$ (analogous to (53)) is doubtful. To address this, the behavior of $H(x,y)$ is proposed to be studied along generic line segments.

Consider a line segment of the form $y = mx + b$ starting at some point $(x_0, y_0) \in \mathbb{R}_+^2$ as shown in Fig. 17. A parameter r is used to represent a generic location (x_r, y_r) on this line

as $(x_r, y_r) = (x_0 + r, y_0 + mr)$ where r have been introduced exploiting the gradient m of the line segment:

$$\frac{y_r - y_0}{x_r - x_0} = m \implies \frac{y_r - y_0}{m} = \frac{x_r - x_0}{1} = r. \quad (56)$$

A rational function $h(r)$ can now be defined as

$$h(r) \triangleq H(x_0 + r, y_0 + mr) = \frac{F(x_0 + r, y_0 + mr)}{G(x_0 + r, y_0 + mr)} = \frac{f(r)}{g(r)} \quad (57)$$

to represent the $H(x,y)$ along the interested line segment.

The parameter r is constrained such that $r \in \mathcal{U} \triangleq [-x_0, \frac{-y_0}{m}]$ to limit the line segment to \mathbb{R}_+^2 . This allows $h(r)$ to fall directly into the category of rational functions discussed before (i.e., in Lemma 3 and in Remark 7).

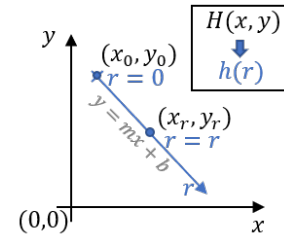


Fig. 17: $H(x,y)$ along the line $y = mx + b$

Theorem 3: The rational function $h(r)$, $r \in \mathcal{U}$ defined in (57) is convex (or concave) if $\Delta_h(r_0) > 0$ (or $\Delta_h(r_0) < 0$), where $r_0 \in \mathcal{U}$ and $\Delta_h(r)$ is defined in (52).

Proof: According to (57) and \mathcal{U} defined above, the denominator polynomial $g(r) = G(x_0 + r, y_0 + mr) > 0$ for all $r \in \mathcal{U}$ as $C_7 \geq 0, C_8 \geq 0$ and $C_9 > 0$ in (55).

Since $g(r)$ and $f(r)$ are polynomials of degree 1 and 2 respectively, they satisfy the condition (51). Thus, Lemma 3 is applicable for $h(r)$ (defined in (57)). Hence, its convexity will depend on the condition $\Delta_h(r_0) > 0$. ■

It is worth pointing out that $\Delta_h(r)$ is in fact independent of r as $\Delta'_h(r) = 0, \forall r \in \mathcal{U}$ (see the last step of the proof of Lemma 3 and (51)). However, it will depend on other parameters (found in (55)) including x_0, y_0 and m . For example, when the line segment defined by $x_0 = 0, y_0 = 0, m = 0$ (i.e., the x -axis) is used, $\Delta_h(r) = 2FG^2 - 2DGK + 2AK^2, \forall r \in \mathbb{R}_+$.

In the introduced parametrization scheme above, the parameter r represents the distance along the x axis from x_0 (projected from the line segment $y = mx + b$). However, if $H(x,y)$ needs to be studied along the y axis (from y_0 projected from a line segment $x = ny + c$), using

$$\frac{y_r - y_0}{x_r - x_0} = \frac{1}{n} \implies \frac{y_r - y_0}{1} = \frac{x_r - x_0}{n} = r. \quad (58)$$

is more appropriate as it gives $(x_r, y_r) = (x_0 + nr, y_0 + r)$.

Above Theorem 3 enables determining the optimum $H(x,y)$ value along a known line segment (on \mathbb{R}_+^2) - using the established Lemma 4 for a problem of the form (53). This capability is exploited next.

4. Constrained minimization of $H(x,y)$: The main objective of this discussion is to obtain a closed form solution to a constrained optimization problem of the form

$$\begin{aligned} (x^*, y^*) = & \underset{(x,y)}{\operatorname{argmin}} H(x,y) \\ & x \geq 0, \\ & y \geq 0, \\ & y - \mathbf{P}x \leq \mathbf{L}, \\ & y + \mathbf{Q}x \leq \mathbf{M}, \\ & x \leq \mathbf{N}, \end{aligned} \quad (59)$$

where $H(x,y)$ is a known bivariate rational function of the form (55) and $\mathbf{P}, \mathbf{Q}, \mathbf{L}, \mathbf{M}$ are known positive constants. These constraints define a convex 2-Polytope as shown in Fig. 18. The steps followed to solve the above problem are discussed next.

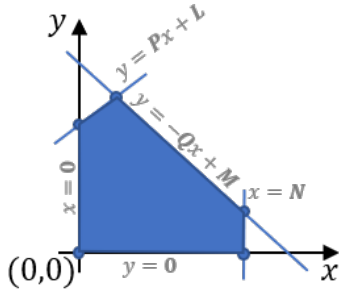


Fig. 18: Feasible space for $H(x,y)$ in (59)

- **Step 1:** The unconstrained version of (59) is considered first. This is solved using the KKT necessary conditions [16] which reveals two equations of generic conics [17]. Therefore, the stationary points of $H(x,y)$ lies at the (four) intersection points of those two conics. The problem of determining the intersection of two conics boils down to solving a quartic equation which has a well known closed form solution [18]. These (four) solutions are computed and stored in a *solution pool* if they satisfy the constraints.

- **Step 2:** Next, the constrained version of (59) is considered. In such a case, it is possible for (x^*, y^*) to lie on a constraint. To capture such situations, $H(x,y)$ is optimized along each of the boundary line segments of the feasible space (there are five of them as shown in Fig. 18).

On a selected boundary line segment, the first step is to parametrize $H(x,y)$ to obtain a single variable rational function $h(r)$ (following either (56) or (58)). Then, the next step is to solve the arising convex (or concave) optimization problem (of the form (53)) using Lemma 4. Note that this is enabled by Theorem 3. Finally, the obtained optimum solution is added to the solution pool.

- **Step 3:** The final step is to pick the best solution out of the solution pool (which only contains at most nine candidates solutions). Therefore, this is achieved by directly evaluating $H(x,y)$ and comparing them for each candidate solution.

This approach is computationally cheap and accurate compared to gradient based methods (which are susceptible to local optima). This concludes the discussion on how to solve a generic problem of the form (59).

B. Omitting the denominator of the RHCP objective function

In this section, the case where the RHCP objective function J_H takes the form

$$J_H(X_i(t), U_{ij}; H) = \tilde{J}_i(t, t+w)$$

is investigated where the denominator term w found in the original definition of J_H in (12) is omitted. The main focus here is given to the RHCP³ where now the objective function $J_H^3(u_j, v_j)$ takes the form

$$J_H^3(u_j, v_j) = C_1 u_j^2 + C_2 v_j^2 + C_3 u_j v_j + C_4 u_j + C_5 v_j + C_6.$$

Each coefficient above is same as in (20). In this appendix, it is shown that the above objective function leads to a spurious policy (for j^*).

The first step of RHCP³ (i.e., (8)) can be stated as:

$$\begin{aligned} (u_j^*, v_j^*) = & \underset{(u_j, v_j)}{\operatorname{argmin}} J_H^3(u_j, v_j) \\ & (u_j, v_j) \text{ s.t. (18).} \end{aligned} \quad (60)$$

3. Solving (60) for optimal control (u_j^*, v_j^*) :

- **Class I:** First assume (u_j^*, v_j^*) belongs to the Class 1 defined in (18). Then, $v_j^* = 0$ and (60) takes the form: (which also determines u_j^*)

$$\begin{aligned} u_j^* = & \underset{u_j}{\operatorname{argmin}} J_H^3(u_j, 0) \\ & 0 \leq u_j < \lambda_j. \end{aligned} \quad (61)$$

Lemma 5: The optimal solution for (61) is

$$u_j^* = 0 \quad (62)$$

Proof: Substituting $v_j = 0$ in (20) gives $J_H^3(u_j, 0)$ as

$$J_H^3(u_j, 0) = C_1 u_j^2 + C_4 u_j + C_6. \quad (63)$$

Recall $C_4 \geq 0$, $C_6 \geq 0$ and $C_1 = \frac{1}{2}(\bar{A} - B_j)$.

First, consider the case where $C_1 = 0$. Then, $J_H^3(u_j, 0)$ is linear in u_j . Also it will have a non-negative gradient as $C_4 \geq 0$. Therefore, when $C_1 = 0$, clearly the constrained optimum is at $u_j^* = 0$.

Note that when $C_1 \neq 0$, the unconstrained optimum of $J_H^3(u_j, 0)$ is at $u_j = u_j^\# = \frac{-C_4}{2C_1}$ (using calculus). Also note that due to the quadratic nature of $J_H^3(u_j, 0)$, it should be symmetric around $u_j = u_j^\#$.

As the second case, consider $C_1 > 0$. Then, $J_H^3(u_j, 0)$ is convex and $u_j^\# \leq 0$. Therefore, when $C_1 > 0$, $u_j^* = 0$.

Finally, consider the case where $C_1 < 0$. Then, $J_H^3(u_j, 0)$ is concave and $u_j^\# \geq 0$. In this case, using the aforementioned symmetry, the constrained optimum u_j^* can be written as

$$u_j^* = \begin{cases} \lambda_j & \text{if } 2u_j^\# < \lambda_j, \\ 0 & \text{otherwise,} \end{cases} \quad (64)$$

Now, it is required to prove that the condition $2u_j^\# < \lambda_j$ never occurs (whenever $C_1 < 0$). Using (20), $u_j^\#$ can be written as,

$$u_j^\# = \frac{-C_4}{2C_1} = \frac{\bar{R}(t) + \bar{A}\rho_{ij}}{B_j - \bar{A}} \quad (65)$$

Note that $C_1 < 0 \iff B_j \geq \bar{A}$. Also from (20), $R_i(t) \leq \bar{R}(t)$ and $A_i \leq \bar{A}$. Therefore, the denominator and the numerator of $u_j^\#$ above can be bounded as

$$[\bar{R}(t) + \bar{A}\rho_{ij}] \geq [R_j(t) + A_j\rho_{ij}] \text{ and } (B_j - \bar{A}) \leq (B_j - A_j).$$

The above result gives (also using λ_j, λ_{j0} definitions in (18)),

$$u_j^\# = \frac{\bar{R}(t) + \bar{A}\rho_{ij}}{B_j - \bar{A}} \geq \frac{R_j(t) + A_j\rho_{ij}}{B_j - A_j} = \lambda_{j0} \geq \lambda_j. \quad (66)$$

Therefore, $u_j^\# \geq \lambda_j$ and hence the condition $2u_j^\# < \lambda_j$ in (69) does not hold. Thus, even when $C_1 < 0$, $u_j^\# = 0$. This completes the proof. ■

- Class 2: Now, assume (u_j^*, v_j^*) belongs to the Class 2 defined in (18). Then, $u_j = u_j^* = \lambda_{j0}$ and $0 < v_j \leq \mu_j$. Therefore, (60) takes the form: (which also determines v_j^*)

$$\begin{aligned} v_j^* &= \arg \min_{v_j} J_H^3(\lambda_{j0}, v_j) \\ 0 < v_j &\leq \mu_j \end{aligned} \quad (67)$$

Lemma 6: The optimal solution for (67) is

$$v_j^* = 0^+ \quad (68)$$

where 0^+ is a constant that is arbitrarily closer to 0 but larger.

Proof: Substituting $u_j = \lambda_{j0}$ in (20) gives $J_H^3(\lambda_{j0}, v_j)$ as

$$J_H^3(\lambda_{j0}, v_j) = C_2 v_j^2 + [C_3 \lambda_{j0} + C_5] v_j + [C_1 \lambda_{j0}^2 + C_4 \lambda_{j0} + C_6]. \quad (69)$$

Recall $C_2, C_3, C_5, \lambda_{j0} \geq 0$ and $C_2 = \frac{\bar{A}_j}{2} = \frac{1}{2} \sum_{m \in \mathcal{N}_i \setminus \{j\}} A_m$.

If $C_2 = 0$, the objective $J_H^3(\lambda_{j0}, v_j)$ is linear in v_j . Also its gradient is non-negative. Therefore, when $C_2 = 0$, clearly the constrained optimum is at $v_j^* = 0^+$.

Now, consider the case where $C_2 > 0$. Then $J_H^3(\lambda_{j0}, v_j)$ has its unconstrained optimum is at $v_j = v_j^\#$ where

$$v_j^\# = \frac{-[C_3 \lambda_{j0} + C_5]}{2C_2}$$

(using calculus). Also note that due to the quadratic nature of $J_H^3(\lambda_{j0}, v_j)$, it should also be symmetric around $v_j = v_j^\#$.

Since $C_2 > 0$, $J_H^3(\lambda_{j0}, v_j)$ is convex. Also, $v_j^\# \leq 0$ as $C_3, C_5, \lambda_{j0} \geq 0$. This implies that the constrained optimum is at $v_j^* = 0^+$ even when $C_2 > 0$. This completes the proof. ■

- Combined Result:

Theorem 4: The optimal solution of (60) is $u_j^* = 0$, $v_j^* = 0$, and the optimal cost is $J_H^3(u_j^*, v_j^*) = C_6$.

Proof: Assume the optimal solution of (60) (u_j^*, v_j^*) belongs to Class 1 of (18). Then, Lemma 5 gives that $u_j^* = 0$, $v_j^* = 0$. The corresponding objective function value (using (63)) is

$$[J_H^3(u_j^*, v_j^*)]_{\text{Class1}} = C_6$$

However, if the the optimal solution of (60) is assumed to be in Class 2 of (18), Lemma 6 gives that $u_j^* = \lambda_{j0}$, $v_j^* = 0^+$. The corresponding objective function value (using (69)) is

$$[J_H^3(u_j^*, v_j^*)]_{\text{Class2}} = [C_1 \lambda_{j0}^2 + C_4 \lambda_{j0} + C_6].$$

If Class 2 to is better performing compared to Class 1,

$$C_1 \lambda_{j0}^2 + C_4 \lambda_{j0} + C_6 \leq C_6.$$

Using $\lambda_{j0} \geq 0$, above condition can be simplified into: $C_1 \lambda_{j0} + C_4 \leq 0$, which is only possible when $C_1 < 0$ as $C_4 \geq 0$. Therefore, this condition can be simplified as: $C_1 < 0$ and,

$$\frac{-C_4}{C_1} \leq \lambda_{j0}.$$

Using (65), the above condition can be written as $2u_j^\# \leq \lambda_j$. however, (66) shows that whenever $C_1 \leq 0$, $u_j^\# \geq \lambda_j$. Thus, clearly the condition $2u_j^\# \leq \lambda_j$ does not hold (A contradiction).

Therefore, the optimal solution of (60) belongs to Class 1 and hence $u_j^* = 0$, $v_j^* = 0$ and $J_H^3(u_j^*, v_j^*) = C_6$. ■

As a result of the above theorem, when the agent a is ready to leave target i at $t = t$, it can compute the optimal trajectory costs $J_H^3(u_j^*, v_j^*)$ for all $j \in \mathcal{N}_i$ by simply using the expression for C_6 where

$$J_H^3(u_j^*, v_j^*) = C_6 = \frac{\rho_{ij}}{2} [2\bar{R}(t) + \bar{A}\rho_{ij}]. \quad (70)$$

4. Solving for optimal next destination j^* : The second step of the RHCP³ (i.e., (9)) is to choose the optimum neighbor j according to

$$j^* = \arg \min_{j \in \mathcal{N}_i} J_H^3(u_j^*, v_j^*). \quad (71)$$

As shown in (1), above j^* defines the ‘‘Action’’ that the agent has to take at $t = t$.

Theorem 5: The optimal solution to (71) is the neighbor $j = j^* \in \mathcal{N}_i$ whom can be reached in a shortest time, i.e.,

$$j^* = \arg \min_{j \in \mathcal{N}_i} \rho_{ij}.$$

Proof: The objective function of the discrete optimization problem (71) is (70). Therefore,

$$j^* = \arg \min_{j \in \mathcal{N}_i} \frac{\rho_{ij}}{2} [2\bar{R}(t) + \bar{A}\rho_{ij}].$$

Note that $\bar{R}(t)$ and \bar{A} terms are independent of j (see (20)). Therefore, the above objective function (i.e., C_6) can be seen as a quadratic function of ρ_{ij} . Also, it is convex and its poles are located at $\rho_{ij} = 0$ and $\rho_{ij} = -\frac{2\bar{R}(t)}{\bar{A}} \leq 0$. Thus, C_6 monotonically increases with ρ_{ij} . As a result, j^* is the neighbor j with the smallest ρ_{ij} value. ■

Above theorem implies that it is optimal to choose the next destination target only based on the (shortest) travel time. This is clearly unfavorable as an agent could converge to oscillate between two targets in the target topology while ignoring others. Hence the importance of the denominator w term included in the RHCP objective function definition (12) is evident.

REFERENCES

- [1] J. Trevathan and R. Johnstone, "Smart Environmental Monitoring and Assessment Technologies (SEMAT) A New Paradigm for Low-Cost, Remote Aquatic Environmental Monitoring," *Sensors (Switzerland)*, vol. 18, no. 7, jul 2018.
- [2] K. Leahy, D. Zhou, C. I. Vasile, K. Oikonomopoulos, M. Schwager, and C. Belta, "Persistent Surveillance for Unmanned Aerial Vehicles Subject to Charging and Temporal Logic Constraints," *Autonomous Robots*, vol. 40, no. 8, pp. 1363–1378, dec 2016.
- [3] X. Meng, A. Houshmand, and C. G. Cassandras, "Multi-Agent Coverage Control with Energy Depletion and Repletion," in *58th IEEE Conf. on Decision and Control*, jan 2019, pp. 2101–2106.
- [4] S. L. Smith, M. Schwager, and D. Rus, "Persistent Monitoring of Changing Environments Using a Robot with Limited Range Sensing," in *IEEE Intl. Conf. on Robotics and Automation*. IEEE, may 2011, pp. 5448–5455.
- [5] V. A. Huynh, J. J. Enright, and E. Frazzoli, "Persistent Patrol with Limited-Range On-Board Sensors," in *49th IEEE Conf. on Decision and Control*, 2010, pp. 7661–7668.
- [6] X. Lin and C. G. Cassandras, "An Optimal Control Approach to The Multi-Agent Persistent Monitoring Problem in Two-Dimensional Spaces," *IEEE Trans. on Automatic Control*, vol. 60, no. 6, pp. 1659–1664, dec 2015.
- [7] N. Zhou, C. G. Cassandras, X. Yu, and S. B. Andersson, "Optimal Threshold-Based Distributed Control Policies for Persistent Monitoring on Graphs," in *American Control Conference*, 2019, pp. 2030–2035.
- [8] S. Welikala and C. G. Cassandras, "Asymptotic Analysis for Greedy Initialization of Threshold-Based Distributed Optimization of Persistent Monitoring on Graphs," in *(Accepted) 21st IFAC World Congress*, 2020.
- [9] N. Zhou, X. Yu, S. B. Andersson, and C. G. Cassandras, "Optimal Event-Driven Multi-Agent Persistent Monitoring of a Finite Set of Data Sources," *IEEE Trans. on Automatic Control*, vol. 63, no. 12, pp. 4204–4217, dec 2018.
- [10] Y. Khazaeni and C. G. Cassandras, "Event-Driven Cooperative Receding Horizon Control for Multi-Agent Systems in Uncertain Environments," *IEEE Trans. on Control of Network Systems*, vol. 5, no. 1, pp. 409–422, mar 2018.
- [11] S. C. Pinto, S. B. Andersson, J. M. Hendrickx, and Christos G. Cassandras, "Multi-Agent Infinite Horizon Persistent Monitoring of Targets with Uncertain States in Multi-Dimensional Environments," in *21st IFAC World Congress (Submitted)*, 2020.
- [12] S. Welikala and C. G. Cassandras, "Asymptotic Analysis for Greedy Initialization of Threshold-Based Distributed Optimization of Persistent Monitoring on Graphs," 2019. [Online]. Available: <http://arxiv.org/abs/1911.02658>
- [13] W. Li and C. G. Cassandras, "A Cooperative Receding Horizon Controller for Multi-Vehicle Uncertain Environments," *IEEE Trans. on Automatic Control*, vol. 51, no. 2, pp. 242–257, feb 2006.
- [14] R. Chen and C. G. Cassandras, "Optimization of Ride Sharing Systems Using Event-driven Receding Horizon Control," in *(Accepted) 21st IFAC World Congress*, 2020.
- [15] Y. Khazaeni and C. G. Cassandras, "Event-Driven Trajectory Optimization for Data Harvesting in Multi-Agent Systems," *IEEE Trans. on Control of Network Systems*, vol. 5, no. 3, pp. 1335–1348, sep 2018.
- [16] D. P. Bertsekas, *Nonlinear Programming*. Athena Scientific, 2016.
- [17] S. Rosenberg, "Conics." [Online]. Available: <http://math.bu.edu/people/sr/GandS/handouts/Chapter6.pdf>
- [18] D. Auckly, "Solving the quartic with a pencil," *American Mathematical Monthly*, vol. 114, no. 1, pp. 29–39, oct 2007.